Astronomy & Astrophysics manuscript no. output
July 19, 2024

VELOcities of CEpheids (VELOCE) II. Systematic search for spectroscopic binary cepheids (Supplementary online-only material)

Shreeya S. Shetye[1,3⋆], Giordano Viviani[1⋆⋆], Richard I. Anderson[1⋆⋆⋆], Nami Mowlavi[2], Laurent Eyer[2], Nancy R. Evans[4], and László Szabados[5]

[1] Institute of Physics, École Polytechnique Fédérale de Lausanne (EPFL), Observatoire de Sauverny, 1290 Versoix, Switzerland
[2] Département d'Astronomie, Université de Genève, Chemin Pegasi 51, 1290 Versoix, Switzerland
[3] Instituut voor Sterrenkunde, KU Leuven, Celestijnenlaan 200D bus 2401, Leuven, 3001, Belgium
[4] Smithsonian Astrophysical Observatory, MS 4, 60 Garden St., Cambridge, MA 02138, USA
[5] Konkoly Observatory, HUN-REN Research Centre for Astronomy and Earth Sciences, MTA Centre of Excellence, Konkoly Thege Miklós út 15-17, H-1121 Budapest, Hungary

Received July 19, 2024; accepted date here

ABSTRACT

This document provides the supporting material for the article titled "VELOcities of CEpheids (VELOCE) II: Systematic Search for Spectroscopic Binary Cepheids" by Shetye et al. (2024). Here we present the full versions of the excerpt tables included in the main article. Detailed descriptions of the methodologies employed can also be found in the main article. This study is based on radial velocity measurements presented in `VELOCE` data release 1 (Anderson et al. 2024), the data is also publicly available at: https://doi.org/10.5281/zenodo.10793507.

Key words. Stars: variables: Cepheids – binaries: visual – Stars: oscillations – distance scale

⋆ e-mail: shreeya.shetye@kuleuven.be
⋆⋆ e-mail: giordano.viviani@epfl.ch
⋆⋆⋆ e-mail: richard.anderson@epfl.ch

1. Basic data about the sample stars

Table 1 is the full version of Table 1 from the main article.

Table 1: Sample of binary Cepheids and candidates from the literature considered here.

Cepheid	*Gaia* DR3 source ID	$\langle m_V \rangle$ (mag)	*Gaia* $\langle m_G \rangle$ (mag)	P_{puls} (d)	Status	References	Evidence	Triple?
Newly discovered spectroscopic binary Cepheids								
AQ Pup	5597379741549105280	8.54	8.32	30.1965	Susp	R1	Trend	Y
ASAS J064540+0330.4				3.0147	New		Orbit	Y
ASAS J064553+1003.8	3350719221309022720	10.78	10.44	2.6801	New		Trend	
ASAS J084951−4627.2	5329675052782690944	11.03	10.85	3.7889	New		Orbit	
ASAS J100814−5856.6	5258280842214814336	11.48	11.40	3.7665	New		Orbit	
ASAS J103158−5814.7	5351436724362450304	11.06	11.08	1.1192	New		Trend	
ASAS J155847−5341.8	5980814424369504256	9.99	9.45	2.8075	New		Trend	
ASAS J174108−2328.5	4116471792510901248	9.55	8.86	3.7797	New		Trend	
ASAS J174603−3528.1	4041107790775862272	10.94	10.31	2.5724	New		Orbit	
β Dor	4757601523650165120	3.76	3.59	9.8427	New		RVTF-Yes	
DR Vel	5313887130948758016	9.25	8.94	11.1995	New		Trend	
FO Car	5241780677399802624	10.96	10.35	10.3569	New		Orbit	Y
GX Car	5257664497238811776	9.42	9.09	7.1969	New		Orbit	
IT Car	5337191279937200256	7.9	7.82	7.5330	New		Orbit	
MY Pup	5506374096132016512	5.65	5.47	5.6941	New		Orbit	
NT Pup	5537860123428416640		11.56	15.5603	New		Orbit	
OX Cam	473293889810320128	10.81	10.06	5.0655	New		Trend	
RY Sco	4041690364529590144	7.51	7.49	20.3267	New		Trend	Y
RY Vel	5355057622307185280	7.86	7.88	28.1742	New		Trend	
SX Vel	5329838158460391296	8.33	8.12	9.5507	New		Trend	
SZ Aql	4267549637851481344	7.92	8.20	17.1409	New		RVTF-Yes	
V0391 Nor	5881995546318024704	8.99	8.66	4.3733	New		Trend	
V0402 Cyg	2060021625508894592	9.87	9.52	4.3649	New		RVTF-Yes	Y
V0407 Cas	2012787293154800896		11.47	4.5661	New		Orbit	Y
V0492 Cyg	2058874388200159872		11.56	7.5780	New		Trend	
V0659 Cen	5868451040512196224	6.49	6.47	5.6240	Susp	R2	Orbit	Y
V0827 Cas	430814876547869440	11.57	10.74	3.1986	New		Trend	Y
V1162 Aql	4190143160245024256	7.81	7.59	5.3762	New		Trend	
V1803 Aql	4319018739208020096	10.35	9.39	8.6281	New		Trend	
V2475 Cyg	2055881689337758336		11.41	11.5557	New		Trend	
VZ Pup	5600052040150252800	10.15	9.34	23.1743	New		Orbit	
X Cyg	1870258975238302208	6.47	6.20	16.3866	New		RVTF-Yes	
First orbital solutions for literature SB1 Cepheids								
BP Cir	5877460679352962048	7.52	7.33	2.3981	Known	R4	Orbit	
FN Vel	5307761545524640256	10.25	9.85	5.3242	Known	VELOCE, R5, R6	Orbit	
MU Cep	2200181111723748224	12.3	11.64	3.7678	Known	VELOCE, R6	Orbit	
R Cru	6054935874795049216	6.42	6.58	5.8257	Known	R7	Orbit	
R Mus	5855468247702904704	6.33	6.23	7.5103	Known	R3	Orbit	
VY Per	459035766618689280	11.32	10.47	5.5319	Known	R24	Orbit	
Literature SB1 confirmed by VELOCE								
α UMi		2.02		3.9720	Known	VELOCE, R32	Orbit [1]	
AD Pup	5614312705966204288	9.99	9.63	13.5976	Susp	R9	Trend	
AH Vel	5519380081746387328	5.76	5.59	4.2272	Known	R3	Trend	
AQ Car	5254662177677566464	8.84	8.64	9.7696	Susp	VELOCE, R10	Trend	
AW Per	174489098011145216	7.51	7.09	6.4638	Known	R11	Trend	Y
AX Cir	5873984023533350400	5.96	5.66	5.2734	Known	R4	Orbit	
CD Cyg	2058374144759464064	8.35	8.59	17.0762	Known	VELOCE, R10	RVTF-Yes	
δ Cep	2200153454733285248	3.75	3.85	5.3663	Known	VELOCE, R12	Orbit	
DL Cas	428620663657823232	8.63	8.58	8.0009	Known	R13, R14	Orbit	
η Aql	4240272953377646592	3.8	3.75	7.1768	Known	R15	RVTF-Yes	
FF Aql	4514145288240593408	5.38	5.17	4.4710	Known	R16	Orbit	Y
FR Car	5337764640889249536	9.64	9.33	10.7169	Known	R17	Trend	
KN Cen	5864135319959353600	9.86	9.24	34.0273	Known	VELOCE, R10	Trend	
LR TrA	5824226655600824704	7.8	7.59	2.4283	Known	R7	Trend	
RS Ori	3368698813404804352	8.42	8.19	7.5669	Known	R18	RVTF-Yes	
RV Sco	6026412893938675712	6.61	6.77	6.0613	Susp	R19	Trend	Y
RW Cam	473043922712140928	8.72	8.23	16.4157	Known	R2	Trend	
RX Aur	200708636406382720	7.62	7.36	11.6248	Known	R20	Trend	
S Mus	5855852527008107008	8.33	5.88	9.6600	Known	R16	Orbit	
S Sge	1820309639468685824	5.36	5.46	8.3821	Known	R20	Orbit	Y
SS CMa	5616601820448126336	9.84	9.56	12.3525	Known	VELOCE, R10	RVTF-Yes	
SU Cyg	2031776202613700480	6.44	6.80	3.8458	Known	R21	Orbit	

Continued on next page

[1] We refer the reader to Anderson (2019) for the detailed orbital solution of α UMi using VELOCE data.

Table 1 – *Continued from previous page*

Cepheid	*Gaia* DR3 source ID	$\langle m_V \rangle$ (mag)	*Gaia* $\langle m_G \rangle$ (mag)	P_{puls} (d)	Status	References	Evidence	Triple?
SY Nor	5884729035255064064	9.77	9.04	12.6452	Known	R2, R14	Orbit	
SZ Cyg	2071433765909167232	9.37	8.95	15.1096	Known	VELOCE, R10	RVTF-Yes	
T Mon	3324535073449061504	5.98	6.12	27.0355	Known	R13, R20	Trend	
TX Mon	3106349738382214144	10.67	10.60	8.7021	Known	R8	Orbit	
U Vul	1825621002188696448	7.16	6.70	7.9907	Known	R17	Orbit	
UX Per	506699870563323264	11.26	11.41	4.5657	Known	R8	Trend	Y
UZ Sct	4104869264724284544	10.91	10.36	14.7475	Susp	R22	Trend	Y
V0340 Ara	5937099633141128448	10.03	9.74	20.8155	Known	R7	RVTF-Yes	
V0916 Aql	4313179507891570304	10.86	10.06	13.4436	Known	R33	RVTF-Yes	
V1334 Cyg	1964855904803120640	5.88	5.72	3.3325	Known	R23	Orbit	Y
VY Sgr	4094007532908816896	11.36	10.50	13.5585	Known	R22	RVTF-Yes	
W Sgr	4050309195613114624	4.69	4.59	7.5951	Known	R16	Orbit	Y
XX Cen	5871922507947292032	7.3	7.62	10.9520	Known	R13	Orbit	
XZ Car	5338036117182452096	8.67	8.31	16.6521	Susp	VELOCE, R10	Trend	
YZ Car	5255254711361371520	8.24	8.39	18.1696	Known	R10, R16	Orbit	
Z Lac	2007201567928631296	8.57	8.19	10.8859	Known	R13	Orbit	Y
Literature SB1 not confirmed by VELOCE								
AA Gem	3430067092837622272	9.91	9.39	11.3037	Known	R8	RVTF-No	
AN Aur	201574982848108416	10.21	10.01	10.2885	Known	R25	RVTF-No	
AV Sgr	4069645924308096512	11.49	10.24	15.3294	Known	R17	RVTF-No	
BB Sgr	4085919765884068736	6.69	6.58	6.6371	Susp	R26	RVTF-No	
BG Cru	6058439910929477120	5.53	5.27	3.3425	Known	R7	RVTF-No	
BG Vel	5324034867356093056	7.69	7.22	6.9239	Susp	VELOCE, R31	RVTF-No	
CS Ori	3330259852538068608	11.29	11.26	3.8891	Known	R8	RVTF-No	
FN Aql	4269036830424588800	7.96	8.01	9.4814	Known	R27	RVTF-No	
RT Aur	3435571660360952704	5.55	5.34	3.7284	Susp	R28	RVTF-No	
RU Sct	4258436301367796480	8.82	8.71	19.7076	Known	R17	RVTF-No	
RZ Vel	5523162573544337408	7.26	6.85	20.4020	Known	VELOCE, R31	RVTF-No	
S Nor	5835124087174043136	6.49	6.18	9.7547	Known	R1	RVTF-No	
SV Per	203496585576324224	8.86	8.70	11.1294	Known	R2	RVTF-No	
TY Sct	4256744187345732224	11	9.90	11.0538	Known	R22	RVTF-No	
TZ Mon	3112475495616980992		10.51	7.4282	Known	R17	RVTF-No	
U Sgr	4092905375639902464	6.68	6.43	6.7453	Known	R14	RVTF-No	
VW Cen	5864955727424819200	10.36	9.85	15.0368	Known	R17	RVTF-No	
VY Car	5351161399793209984	6.87	7.34	18.8824	Susp	VELOCE, R10	RVTF-No	
WZ Sgr	4094784475310672128	7.45	7.68	21.8494	Known	R30	RVTF-No	
X Lac	2004036486267748352	8.42	8.12	5.4454	Known	R20	RVTF-No	
X Pup	5620098679741674496	8.46	8.35	25.9697	Susp	VELOCE, R10	RVTF-No	
XX Car	5238808628736339584	9.42	9.08	15.7052	Known	R30	RVTF-No	
YZ Aur	188724234539584256	10.24	9.88	18.1943	Known	R8	RVTF-No	
YZ Sgr	4099189015819292800	7.02	7.01	9.5539	Known	R17	RVTF-No	

Notes. Identifiers and magnitudes were compiled from SIMBAD, *Gaia* mean G-band magnitudes from the *Gaia* archive, and pulsation periods from Paper I. Column "Status" indicates whether a star's SB1 nature was newly discovered ("New"), or previously known or suspected ("Known" or "Susp"). Stars listed as Susp among newly discovered SB1 systems were considered tentative previously. References to previous studies are abbreviated using alphanumeric codes as follows. R1: Evans & Udalski (1994), R2: Evans (1994), R3: Lloyd Evans (1982), R4: Petterson et al. (2004), R5: Kovtyukh et al. (2015), R6: Anderson (2013), R7: Szabados (2003), R8: Szabados & Pont (1998), R9: Szabados et al. (2013b), R10: Anderson et al. (2016), R11: Griffin (2016), R12: Anderson et al. (2015), R13: Evans (1995), R14: Bersier et al. (1994), R15: Evans (1991), R16: Gallenne et al. (2019), R17: Szabados (1996), R18: Evans et al. (1990), R19: Evans (1992), R20: Gorynya et al. (1996a), R21: Wahlgren & Evans (1998), R22: Pont et al. (1994), R23: Gallenne et al. (2013), R24: Szabados (1992), R25: Madore (1977), R26: Gieren (1982), R27: Szabados et al. (2014), R28: Turner et al. (2007), R29: Russo et al. (1981), R30: Bersier (2002), R31: Szabados et al. (2013a), R32: Anderson (2019), R33: Gorynya et al. (1996b). The stars with "VELOCE" in the "References" column are cases where VELOCE data was previously used to establish the binarity or the orbit. Column "Evidence" states whether we determine a combined model for orbit and pulsation ("Orbit"), determine a trend in the pulsation residuals ("Trend"), or whether template fitting involving literature RV data indicates a time-variable v_γ ("RVTF-Yes") or not ("RVTF-No"). The last column "Triple?" indicates whether the star is likely part of a triple system, usually involving a visually resolved companion.

2. Full orbital solutions

This section presents the results obtained by fitting full orbital solutions to the RV time-series. We determined complete orbital solutions for 33 stars (including three tentative orbital fits). In Section 2.1 we provide the results based on `VELOCE` data alone, followed by results based on combined `VELOCE` and (zero-point offset-corrected) literature RVs in Section 2.2. Tables 2 and 3 distinguish these solution types using the tags "V" and "V+L", respectively. Lastly, Tables 2 and 3 are the full versions of Tables 3 and 4 from the main article.

Table 2: Orbital elements of the new spectroscopic binary Cepheids' orbits presented in this work. Table notes are provided at the end of Table 3.

Cepheid	P_{puls}	T_0-2.4M	data	P_{orb} (d)	e	K (km s^{-1})	$a \sin i$ (au)	fmass	ω (deg)	M_1	rms
	(d)			$\sigma_{P_{orb}}$	σ_e	σ_K	σ_{asini}	σ_{fmass}	$\sigma_{argperi}$	$M_\odot$	(km s^{-1})
			New orbits from current work								
ASAS	3.0147	59 013.59	V	901.18	0.444	5.810	0.4313	1.3×10^{-2}	203.14	5.0	0.13
J064540+0330.4		2.67	3	2.81	0.011	0.059	0.0052	4.7×10^{-4}	1.39		
ASAS	3.7889	57 854.64	V	1578.27	0.432	14.760	1.9314	3.9×10^{-1}	145.44	4.9	0.26
J084951−4627.2		6.60	4	3.41	0.005	0.158	0.0218	1.3×10^{-2}	1.37		
ASAS	3.7665	58 067.71	V	2458.57	0.454	13.777	2.7740	4.7×10^{-1}	20.85	4.2	0.23
J100814−5856.6		1.79	5	1.22	0.004	0.083	0.0179	9.1×10^{-3}	0.29		
ASAS	2.5724	58 980.80	V	2302.73	0.358	4.145	0.8192	1.4×10^{-2}	344.02	4.9	0.22
J174603−3528.1		97.27	6	41.74	0.153	1.476	0.2966	1.5×10^{-2}	13.49		
FN Vel	5.3242	56 407.87	V	471.79	0.218	21.908	0.9273	4.8×10^{-1}	42.07	6.4	0.16
		0.36	9	0.06	0.001	0.025	0.0011	1.7×10^{-3}	0.21		
FO Car	10.3569	58 244.27	V	1667.57	0.378	14.932	2.1194	4.6×10^{-1}	85.26	6.1	0.16
		2.99	10	2.82	0.002	0.030	0.0059	3.1×10^{-3}	0.59		
		58 244.89	V+L	1662.25	0.378	14.911	2.1096	4.5×10^{-1}	85.72		0.58
		1.81	34	1.57	0.002	0.025	0.0044	2.6×10^{-3}	0.27		
GX Car	7.1969	56 836.78	V	2630.34	0.038	5.034	1.2163	3.5×10^{-2}	6.69	5.6	0.12
		32.46	11	5.82	0.003	0.017	0.0049	3.6×10^{-4}	4.44		
IT Car	7.5330	59 460.47	V	1249.33	0.584	8.934	0.8327	4.9×10^{-2}	116.70	6.0	0.09
		0.66	12	0.79	0.002	0.025	0.0028	4.9×10^{-4}	0.20		
MU Cep	3.7678	56 071.16	V	2028.14	0.434	6.880	1.1552	5.0×10^{-2}	10.29	5.8	0.19
		3.02	13	2.70	0.004	0.035	0.0066	8.3×10^{-4}	0.68		
MY Pup	5.6941	57 936.81	V	2082.44	0.103	0.671	0.1277	6.4×10^{-5}	80.71	5.0	0.12
		431.76	14	54.54	0.052	0.023	0.0056	6.9×10^{-6}	84.82		
		57 974.90	V+L	2186.14	0.141	0.654	0.1300	6.1×10^{-5}	91.59		0.31
		39.93	35	10.44	0.010	0.008	0.0018	2.4×10^{-6}	7.95		
NT Pup	15.5603	56 679.13	V	3653.65	0.466	8.838	2.6268	1.8×10^{-1}	205.92	9.7	0.41
		6.43	2	17.42	0.005	0.052	0.0214	3.7×10^{-3}	0.64		
R Cru	5.8257	57 292.65	V	237.42	0.017	1.029	0.0224	2.7×10^{-5}	205.14	5.5	0.16
		26.80	15	0.14	0.013	0.012	0.0003	9.5×10^{-7}	34.00		
		57 158.38	V+L	237.62		0.999	0.0218	2.5×10^{-5}			0.25
		0.17	36	0.03		0.003	0.0001	2.5×10^{-7}			
V0407 Cas	4.5661	57 445.28	V	498.36	0.307	1.864	0.0812	2.9×10^{-4}	102.46	5.3	0.09
		11.76	21	0.83	0.041	0.153	0.0068	7.2×10^{-5}	12.37		
VY Per	5.5319	57 861.60	V	806.18	0.382	3.835	0.2626	3.7×10^{-3}	108.71	5.0	0.08
		10.45	23	0.78	0.015	0.083	0.0060	2.5×10^{-4}	2.32		
		57 858.11	V+L	805.08	0.369	3.928	0.2702	4.1×10^{-3}	109.34		0.45
		15.58	46	0.63	0.020	0.127	0.0091	4.1×10^{-4}	4.17		
VZ Pup	23.1743	58 234.08	V	3674.13	0.151	2.036	0.6798	3.1×10^{-3}	128.74	8.3	0.38
		241.00	24	222.86	0.036	0.054	0.0452	3.2×10^{-4}	9.43		
		58 184.47	V+L	4026.33	0.251	2.112	0.7566	3.6×10^{-3}	126.95		0.58
		21.25	47	17.82	0.007	0.013	0.0060	7.1×10^{-5}	1.35		
			New "Tentative" orbits from current work								
BP Cir	2.3981	55 730.42	V+L	4339.48	0.779	2.185	0.5463	1.2×10^{-3}	228.69		0.35
		11.60	31	8.49	0.006	0.055	0.0153	9.7×10^{-5}	0.81		
R Mus	7.5103	58 352.07	V+L	4446.72	0.551	1.694	0.5779	1.3×10^{-3}	220.23		1.75
		19.28	37	19.04	0.005	0.009	0.0045	2.6×10^{-5}	1.15		
V0659 Cen	5.6240	52 812.11	V+L	9276.06	0.323	8.260	6.6651	4.6×10^{-1}	182.52		0.86
		81.52	44	130.38	0.052	1.519	1.2358	2.5×10^{-1}	0.90		

Table 3: Orbital elements of VELOCE SB1 Cepheids with literature-known orbits.

Cepheid	P_{puls} (d)	T_0-2.4M	data	P_{orb} (d) $\sigma_{P_{orb}}$	e σ_e	K (km s^{-1}) σ_K	$a \sin i$ (au) σ_{asini}	fmass σ_{fmass}	ω (deg) $\sigma_{argperi}$	M_1 $M_\odot$	rms (km s^{-1})
Update to literature-known SB1s orbits											
AX Cir	5.2734	54 483.59	V+L	6284.51	0.187	10.954	6.2167	8.1×10^{-1}	211.34	5.0	1.76
		33.04	30	12.41	0.009	0.229	0.1311	5.1×10^{-2}	1.21		
δ Cep	5.3663	58 696.03	V	3450.96	0.745	3.012	0.6367	2.9×10^{-3}	242.75	5.0	0.09
		13.61	1	19.57	0.006	0.018	0.0081	9.9×10^{-5}	0.56		
DL Cas	8.0009	58 113.85	V	684.89	0.344	16.656	0.9846	2.7×10^{-1}	25.92	7.1	0.30
		1.00	7	0.21	0.005	0.098	0.0061	5.0×10^{-3}	0.60		
		57 434.67	V+L	684.67	0.341	16.343	0.9668	2.6×10^{-1}	29.25		1.43
		0.99	32	0.06	0.004	0.102	0.0062	5.0×10^{-3}	0.61		
FF Aql	4.4710	58 253.28	V	1433.20	0.050	4.788	0.6300	1.6×10^{-2}	304.87	5.8	0.14
		35.41	8	5.66	0.011	0.028	0.0045	3.0×10^{-4}	6.55		
		58 302.23	V+L	1431.70	0.068	4.877	0.6403	1.7×10^{-2}	317.41		3.68
		7.86	33	0.55	0.004	0.014	0.0019	1.5×10^{-4}	2.02		
S Mus	9.6600	56 663.89	V	505.27	0.087	14.786	0.6842	1.7×10^{-1}	197.92	6.0	0.09
		1.39	16	0.09	0.002	0.019	0.0009	6.5×10^{-4}	0.96		
		56 152.57	V+L	505.16	0.081	14.777	0.6839	1.7×10^{-1}	194.11		2.18
		2.43	38	0.09	0.004	0.020	0.0009	6.8×10^{-4}	1.75		
S Sge	8.3821	58 141.06	V	675.84	0.236	15.525	0.9371	2.4×10^{-1}	200.47	6.0	0.25
		2.16	17	0.27	0.003	0.071	0.0044	3.3×10^{-3}	0.98		
		57 468.20	V+L	676.01	0.248	15.626	0.9407	2.4×10^{-1}	201.53		1.98
		1.19	39	0.06	0.003	0.050	0.0031	2.4×10^{-3}	0.54		
SU Cyg	3.8458	56 395.19	V+L	548.26	0.342	29.444	1.3944	1.2	220.48	5.2	3.28
		1.74	40	0.10	0.005	0.218	0.0107	2.8×10^{-2}	1.57		
SY Nor	12.6452	57 784.70	V	551.92	0.001	15.329	0.7777	2.1×10^{-1}	255.16	6.8	0.24
		321.35	18	0.77	0.003	0.055	0.0030	2.2×10^{-3}	196.34		
		57 945.67	V+L	551.96		15.335	0.7781	2.1×10^{-1}			0.49
		0.16	41	0.06		0.013	0.0007	5.3×10^{-4}			
TX Mon	8.7021	59 204.55	V	1602.20	0.583	11.985	1.4338	1.5×10^{-1}	295.49	7.1	0.18
		4.50	19	2.47	0.004	0.124	0.0157	5.0×10^{-3}	0.45		
		57 599.41	V+L	1606.98	0.585	11.980	1.4359	1.5×10^{-1}	295.12		0.73
		1.91	42	0.91	0.002	0.048	0.0061	1.9×10^{-3}	0.26		
U Vul	7.9907	59 935.90	V	2528.77	0.551	3.154	0.6120	4.8×10^{-3}	1.37	7.1	0.12
		5.28	20	8.57	0.005	0.045	0.0094	2.2×10^{-4}	0.69		
		57 404.92	V+L	2521.23	0.555	3.133	0.6039	4.6×10^{-3}	359.36		1.02
		2.47	29	0.94	0.003	0.017	0.0036	8.1×10^{-5}	0.33		
V1334 Cyg	3.3325	57 172.49	V	1947.79	0.229	14.208	2.4763	5.3×10^{-1}	227.11	5.2	0.05
		1.74	22	2.08	0.001	0.037	0.0070	4.2×10^{-3}	0.37		
		57 186.80	V+L	1931.17	0.236	14.492	2.4999	5.6×10^{-1}	231.09		0.89
		2.62	45	1.12	0.003	0.049	0.0087	5.8×10^{-3}	0.56		
W Sgr	7.5951	58 121.40	V	2006.30	0.272	1.507	0.2675	6.3×10^{-4}	317.92	5.5	0.20
		26.28	25	17.78	0.039	0.013	0.0045	2.8×10^{-5}	4.43		
XX Cen	10.9520	58 211.33	V	722.44	0.295	5.396	0.3424	1.0×10^{-2}	283.11	6.4	0.12
		1.66	26	0.42	0.004	0.026	0.0017	1.6×10^{-4}	0.92		
YZ Car	18.1696	57 936.96	V	827.20	0.029	10.380	0.7889	9.6×10^{-2}	352.67	7.4	0.24
		38.68	27	1.21	0.004	0.062	0.0048	1.7×10^{-3}	16.68		
		57 120.73	V+L	830.02		10.191	0.7776	9.1×10^{-2}			1.87
		0.15	43	0.11		0.009	0.0007	2.3×10^{-4}			
Z Lac	10.8859	58 534.56	V	382.77	0.014	10.774	0.3790	5.0×10^{-2}	65.01	8.0	0.10
		54.21	28	0.14	0.020	0.322	0.0113	4.4×10^{-3}	43.45		

Notes. The pulsation period and epoch are retrieved after the RV fitting following the method described in Paper 1. In column 4, "V" denotes when the orbits were strictly fitted with VELOCE data alone, while "V+L" denotes when the orbit was fitted using the combination of v_γ residuals from VELOCE and literature datasets (See Section 3.2 of the main article for more details about the methods). The second row in the "data" column contains links to the orbital fit figures presented in the paper. The next columns list the different orbital elements, namely, orbital period (P_{orb}), eccentricity (e), semi-amplitude (K), projected semi-major axis (asini), mass function (fmass), argument of periastron (ω). We estimated the individual Cepheid masses (M_1) using period-mass relations based on Geneva stellar evolution models (Ekström et al. 2012), our method was similar to the one described in Anderson et al. (2016). The last column presents the "rms" (root mean square) of the fit between the Fourier+Keplerian model and the RV data for V orbits and between the keplerian model and epoch residuals for V+L orbits.

2.1. Orbits from VELOCE data alone (V)

From Figure 1 to 28, we present all the orbital fits obtained using VELOCE data alone. The orbital fittings were derived using the method described in Section 3.2 of the main article.

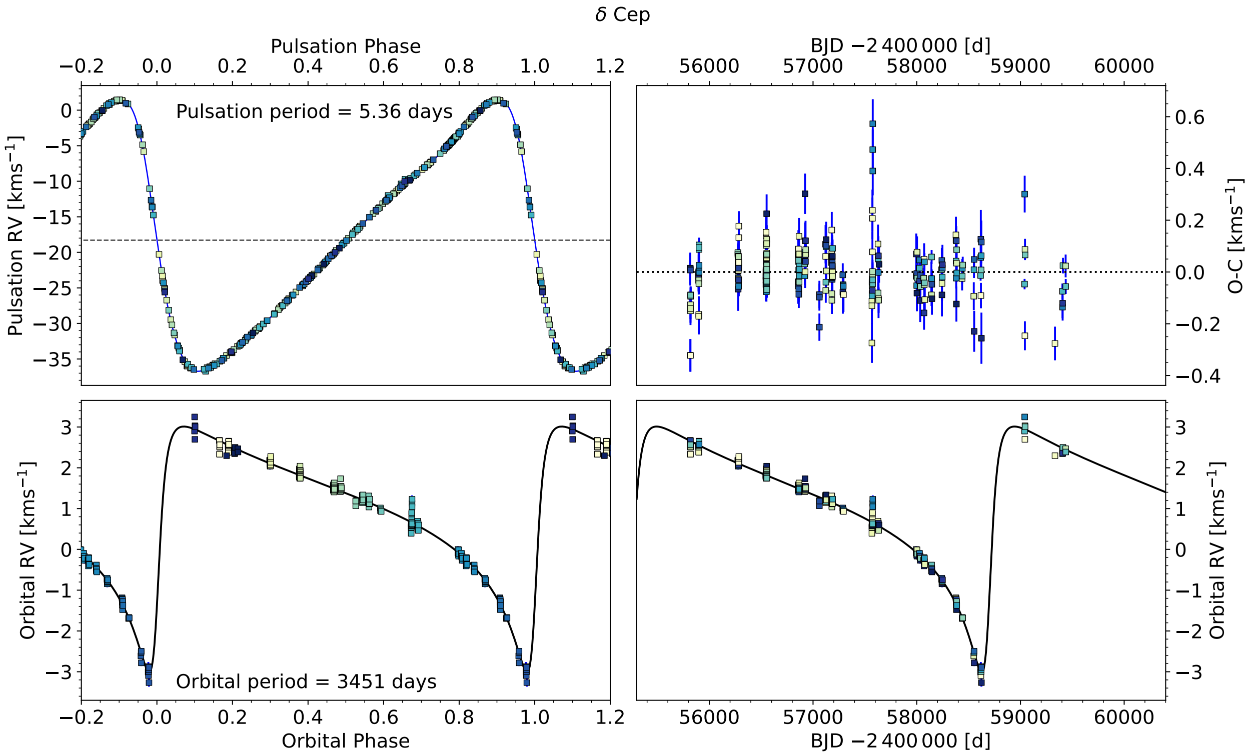

Fig. 1: Pulsation and orbital fit of the naked-eye Cepheid prototype δ Cephei. Left top: pulsation RV variability where the systemic velocity, $v_{\gamma,0}$ is indicated by a dashed line. Right top: residuals after fitting the Fourier series and Keplerian orbit against observation date. Left bottom: phase-folded orbital RV variation against orbital phase. Right bottom: orbital RV variation versus the observation date.

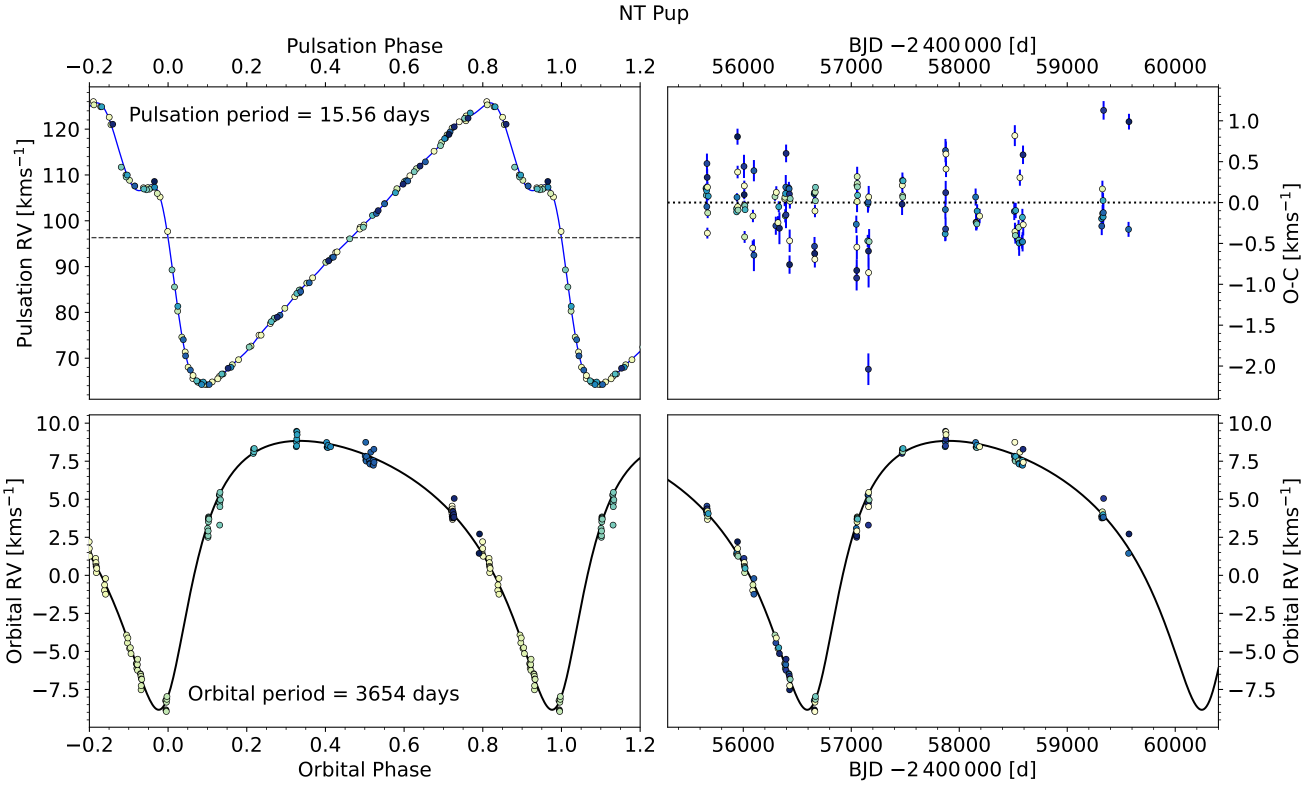

Fig. 2: Pulsation and orbital fit of one of the faintest binaries in our sample, NT Puppis. The figure description is the same as Figure 1.

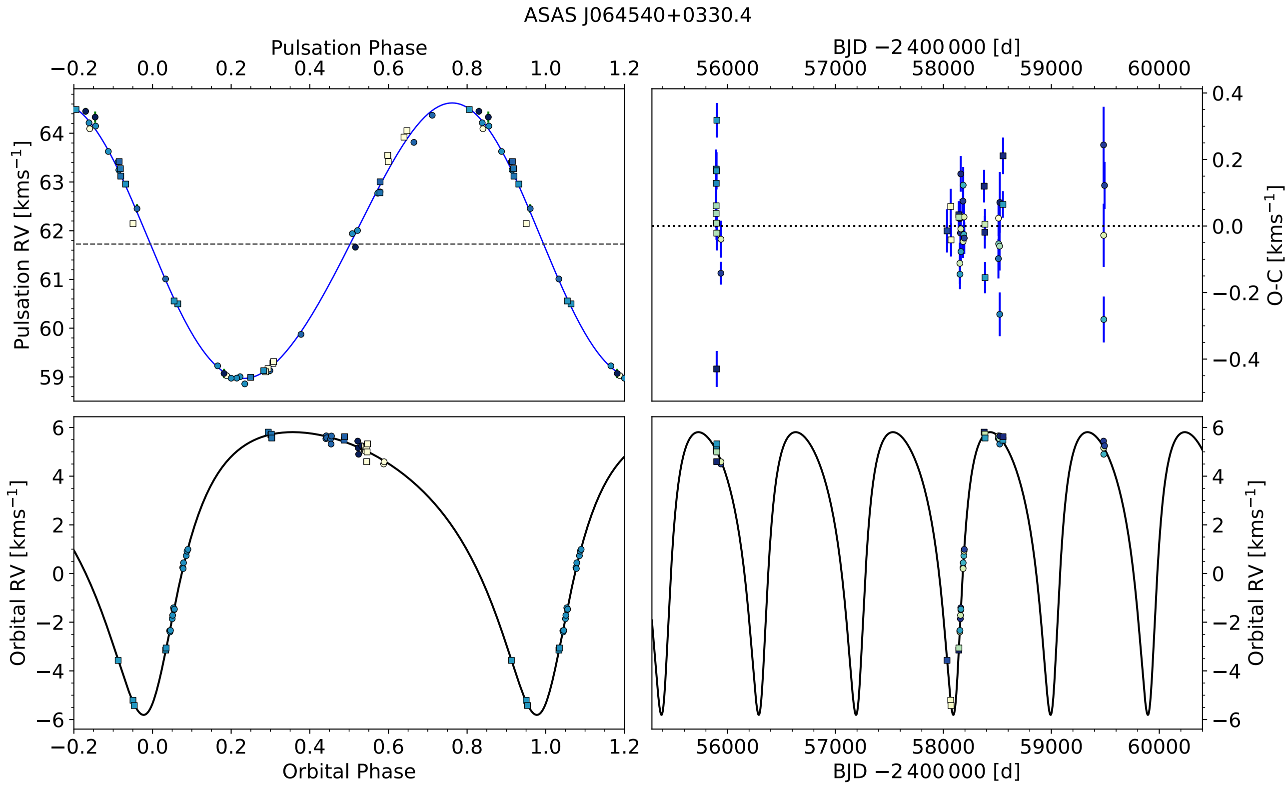

Fig. 3: Pulsational and orbital fit of ASAS J064540+0330.4. The figure description is the same as Figure 1.

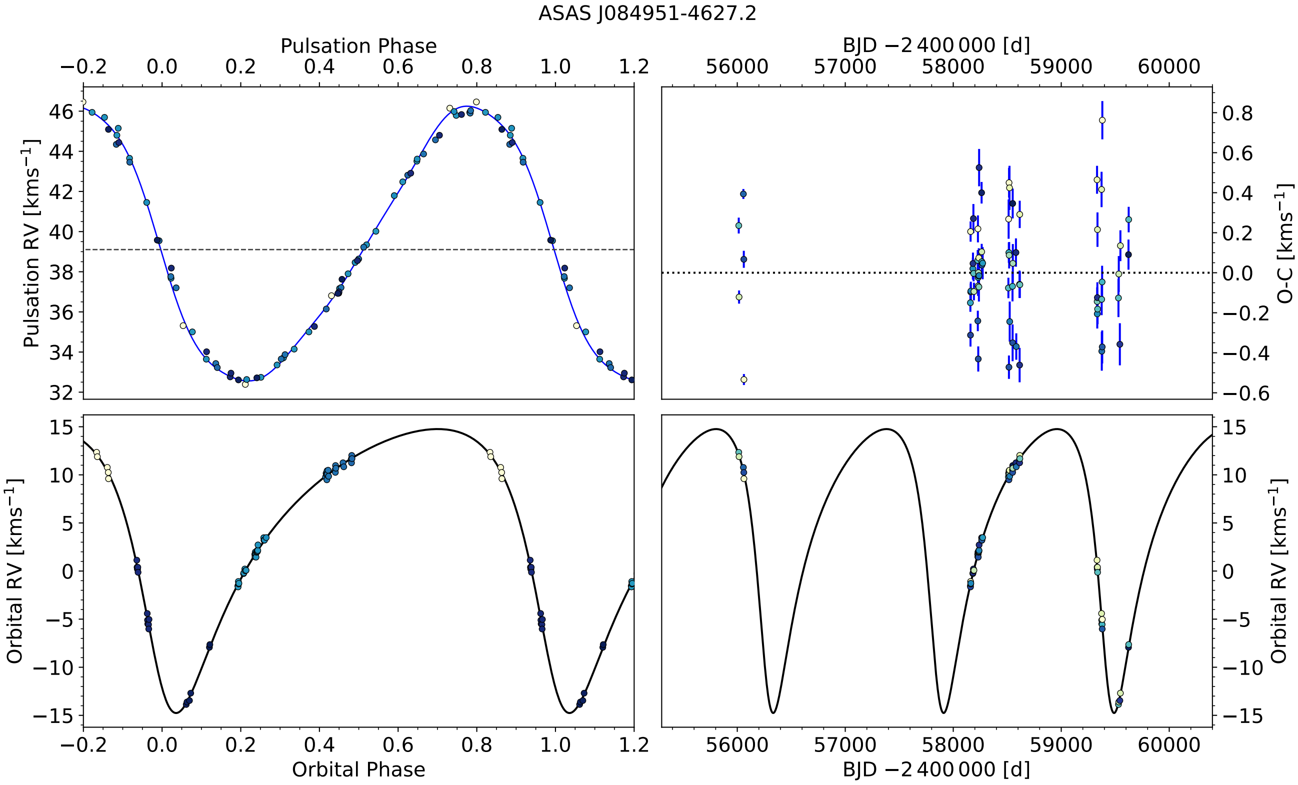

Fig. 4: Pulsational and orbital fit of ASAS J084951-4627.2. The figure description is the same as Figure 1. The pulsational RV curve amplitude modulation is apparent in the top left panel.

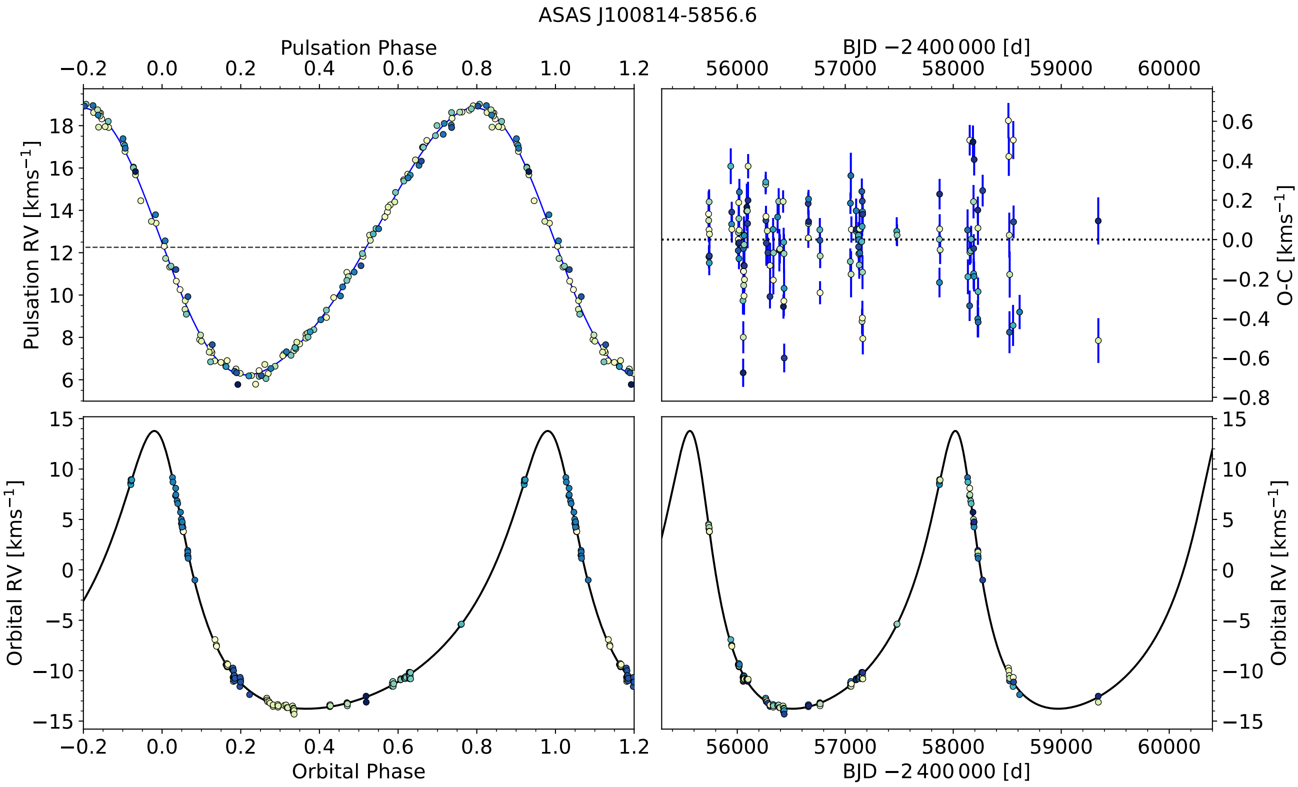

Fig. 5: Pulsational and orbital fit of ASAS J100814-5856.6. The figure description is the same as Figure 1.

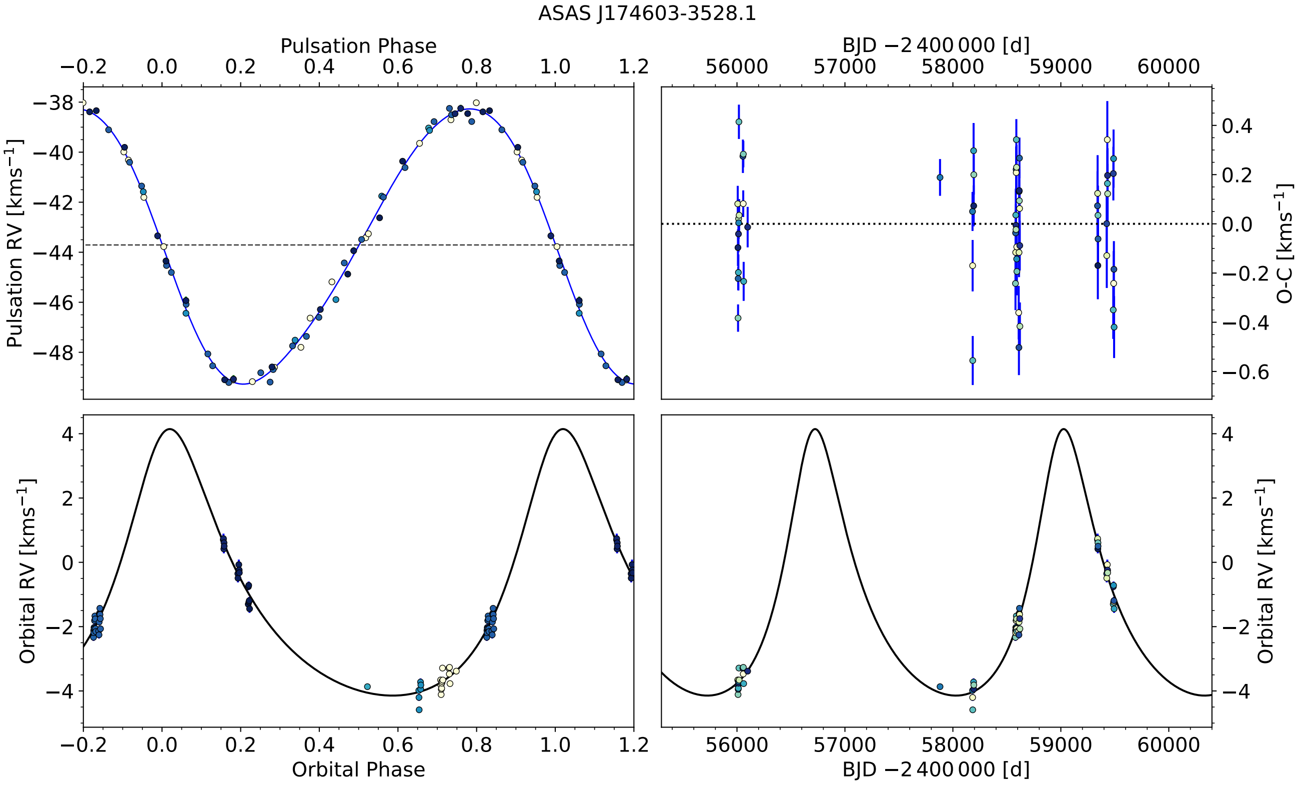

Fig. 6: Pulsational and orbital fit of ASAS J174603-3528.1. The figure description is the same as Figure 1.

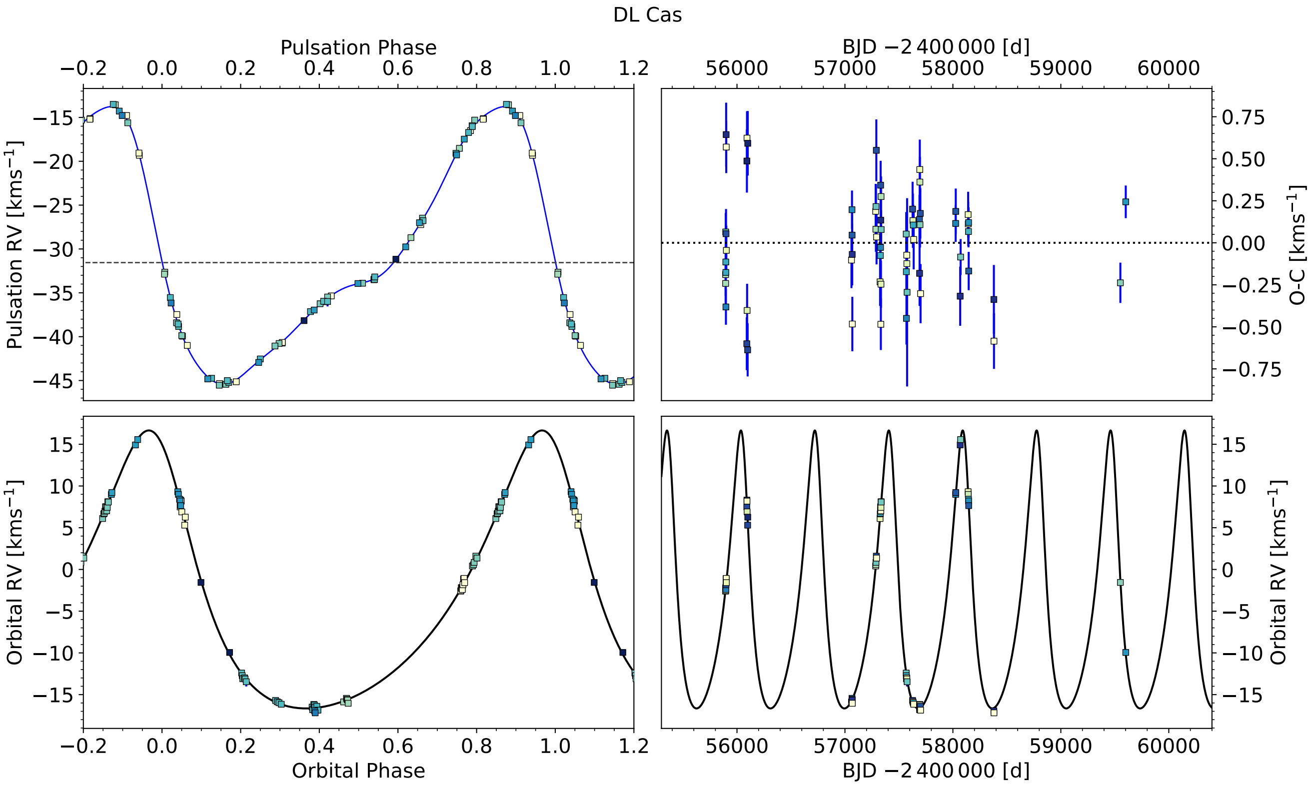

Fig. 7: Pulsational and orbital fit of DL Cas. The figure description is the same as Figure 1.

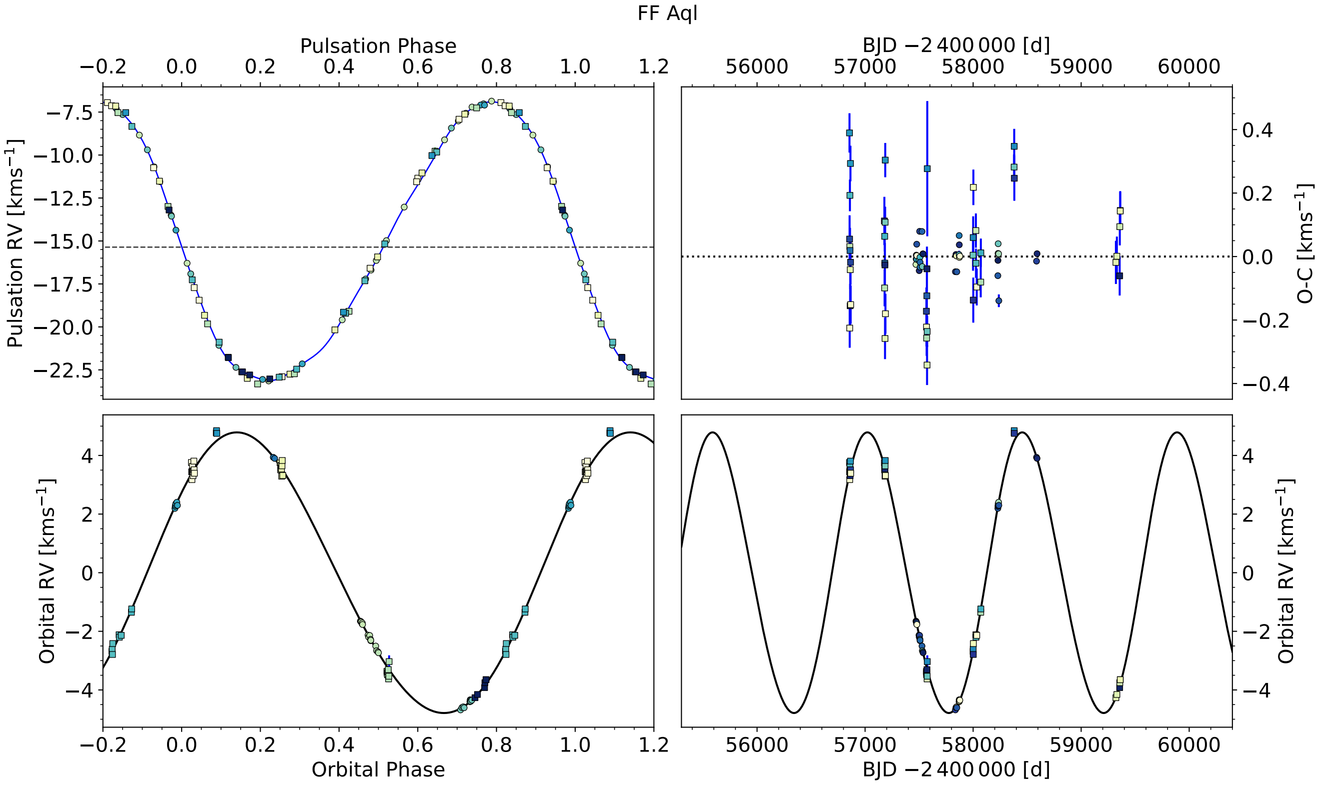

Fig. 8: Pulsational and orbital fit of FF Aql. The figure description is the same as Figure 1.

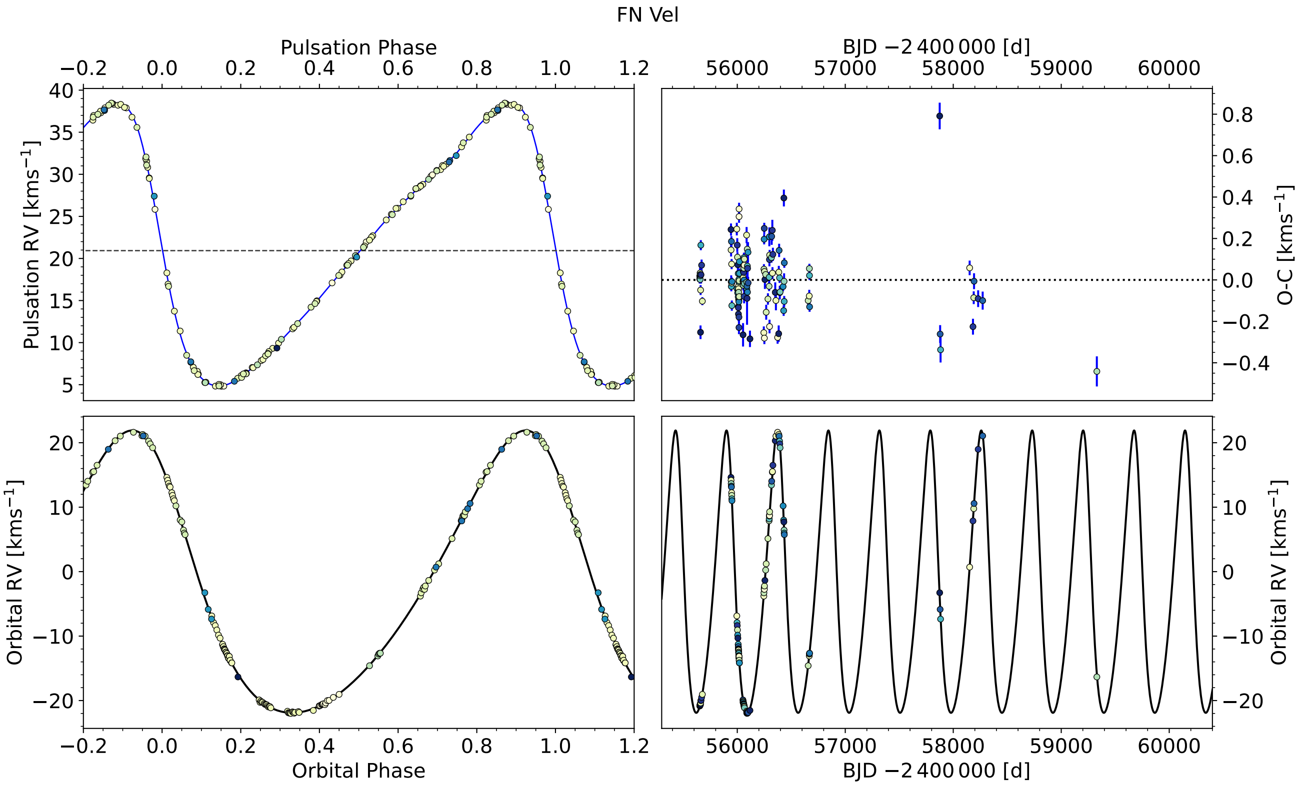

Fig. 9: Pulsational and orbital fit of FN Vel. The figure description is the same as Figure 1.

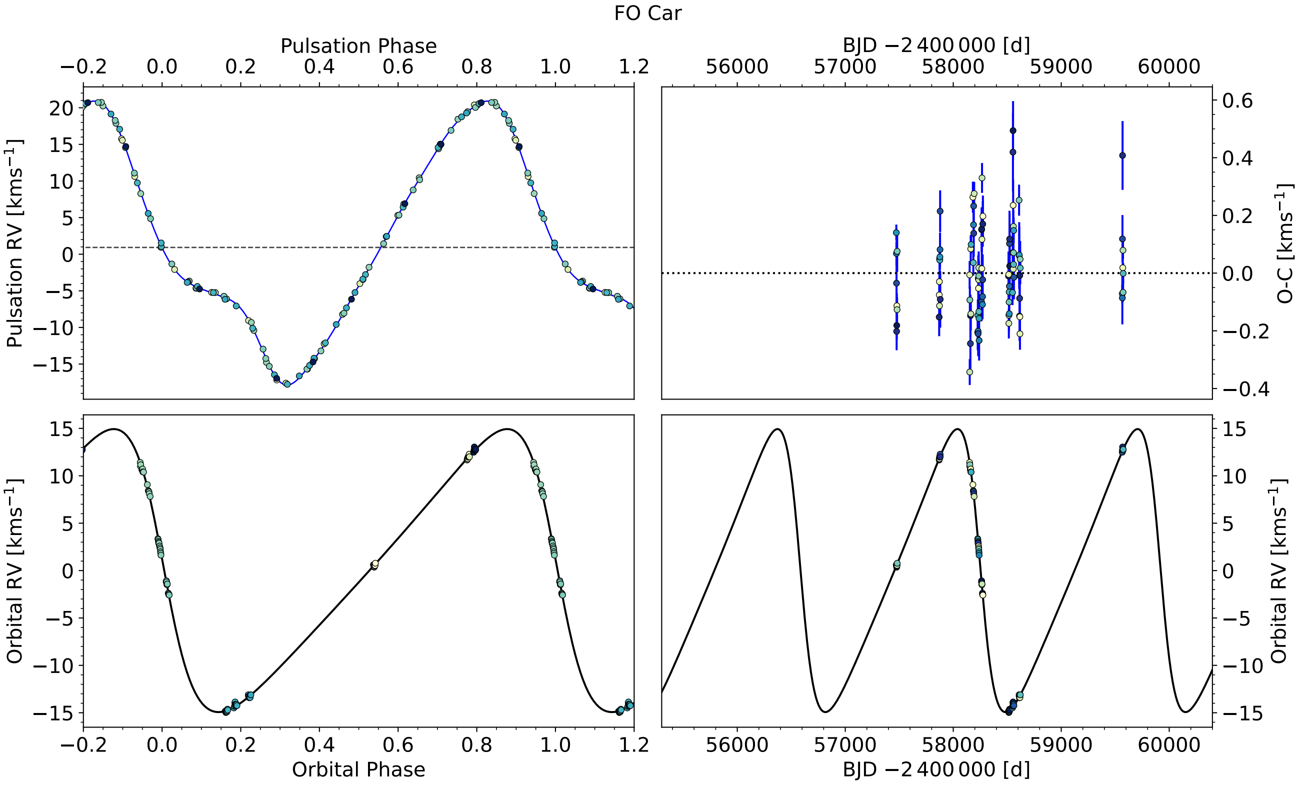

Fig. 10: Pulsational and orbital fit of FO Car. The figure description is the same as Figure 1.

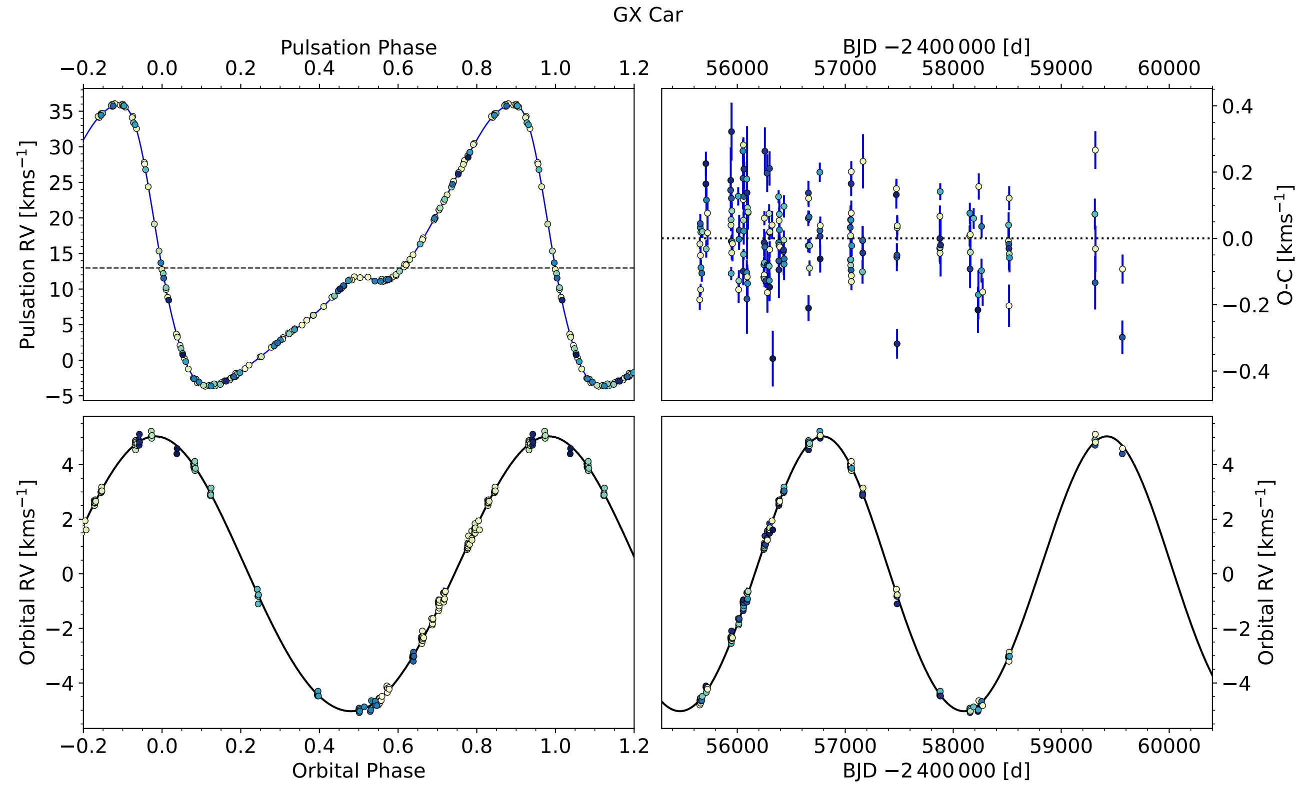

Fig. 11: Pulsational and orbital fit of GX Car. The figure description is the same as Figure 1.

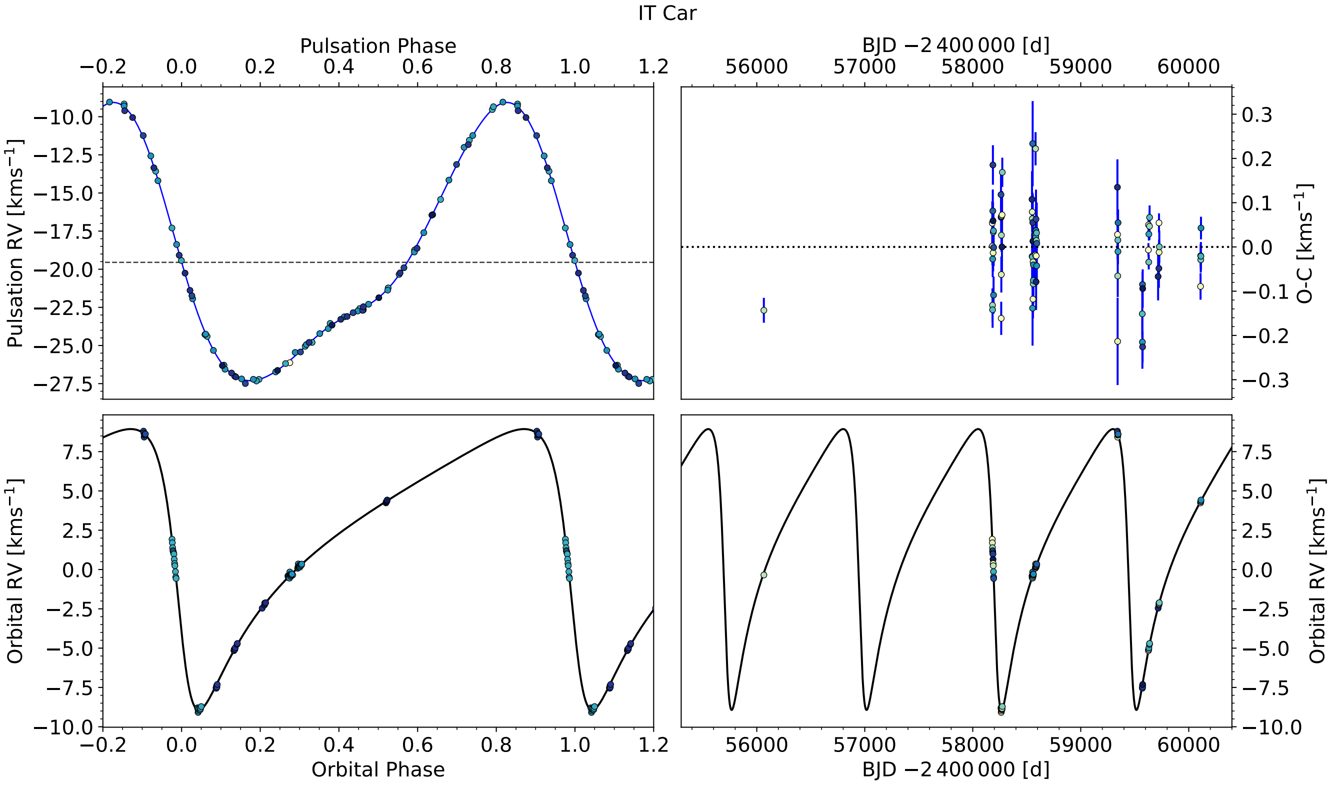

Fig. 12: Pulsational and orbital fit of IT Car. The figure description is the same as Figure 1.

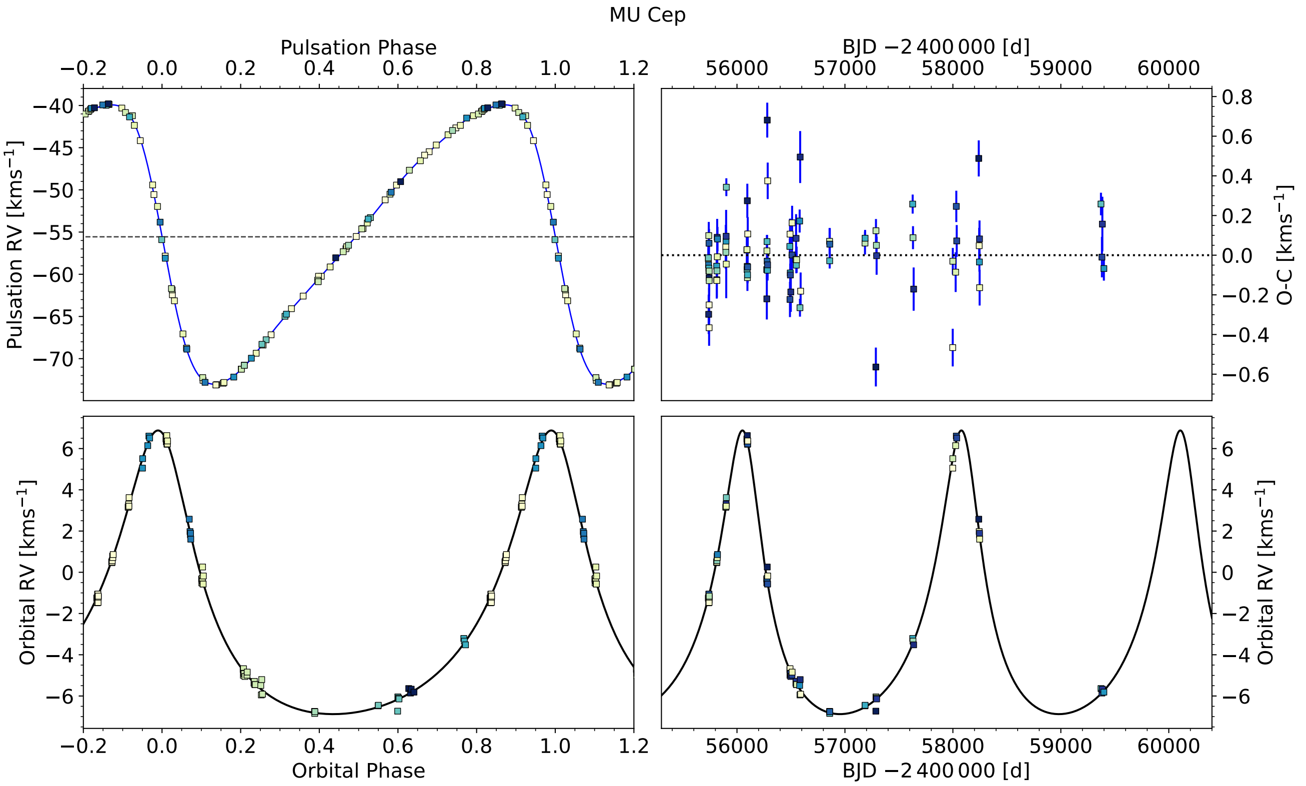

Fig. 13: Pulsational and orbital fit of MU Cep. The figure description is the same as Figure 1.

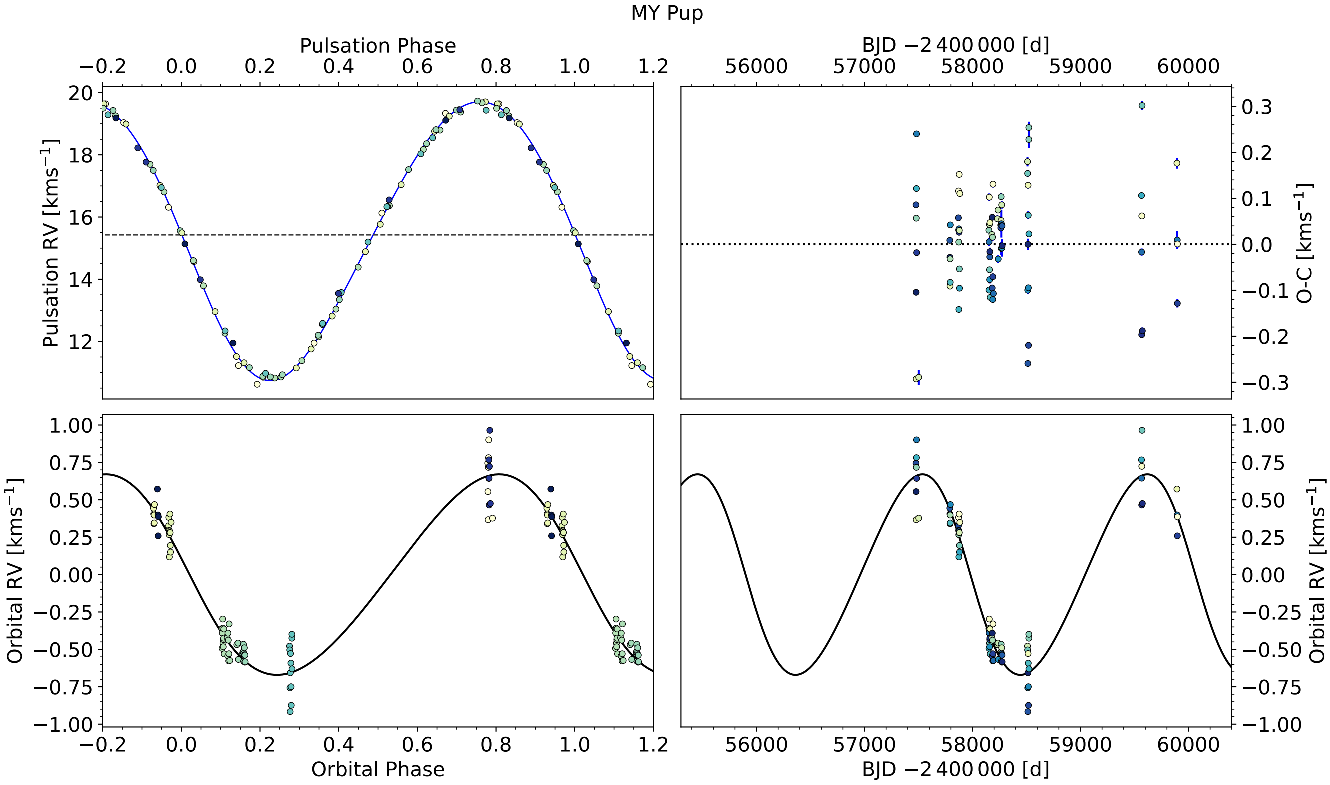

Fig. 14: Pulsational and orbital fit of MY Pup. The figure description is the same as Figure 1.

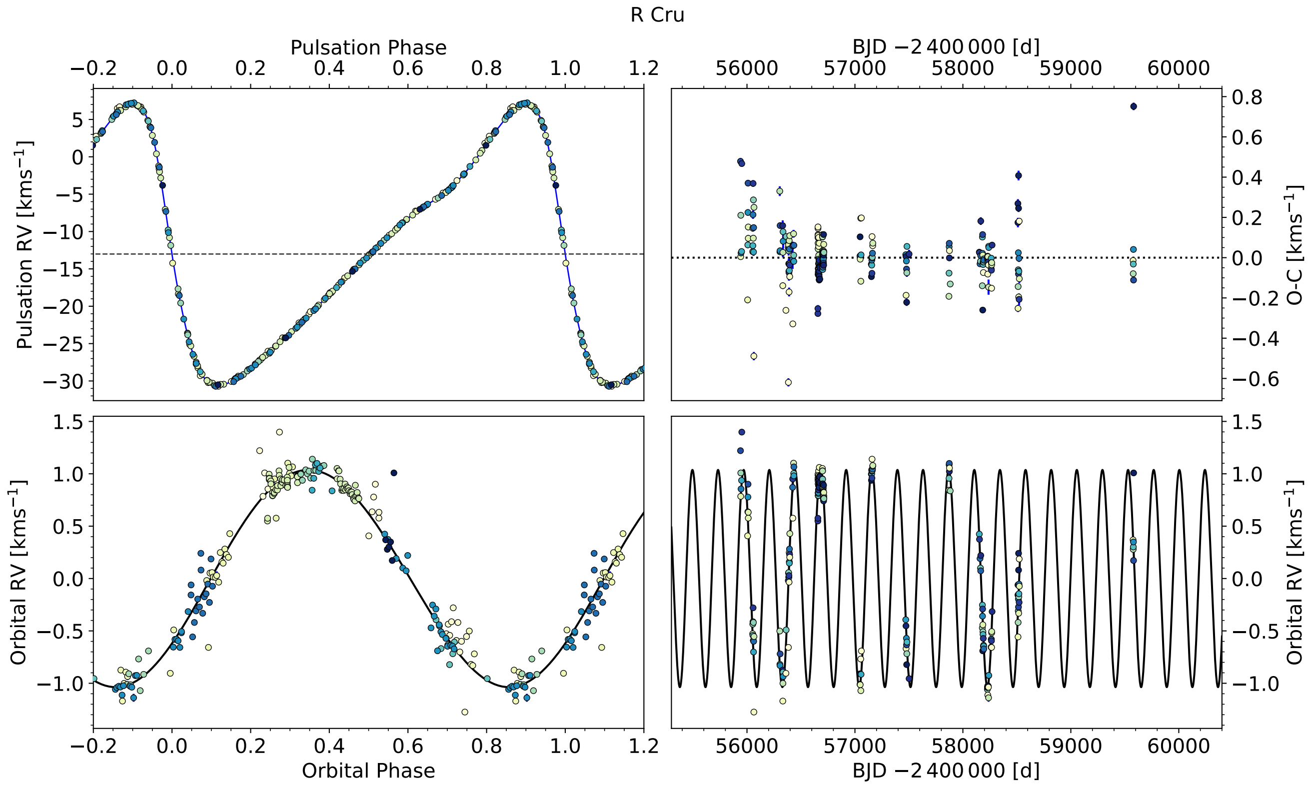

Fig. 15: Pulsational and orbital fit of R Cru. The figure description is the same as Figure 1.

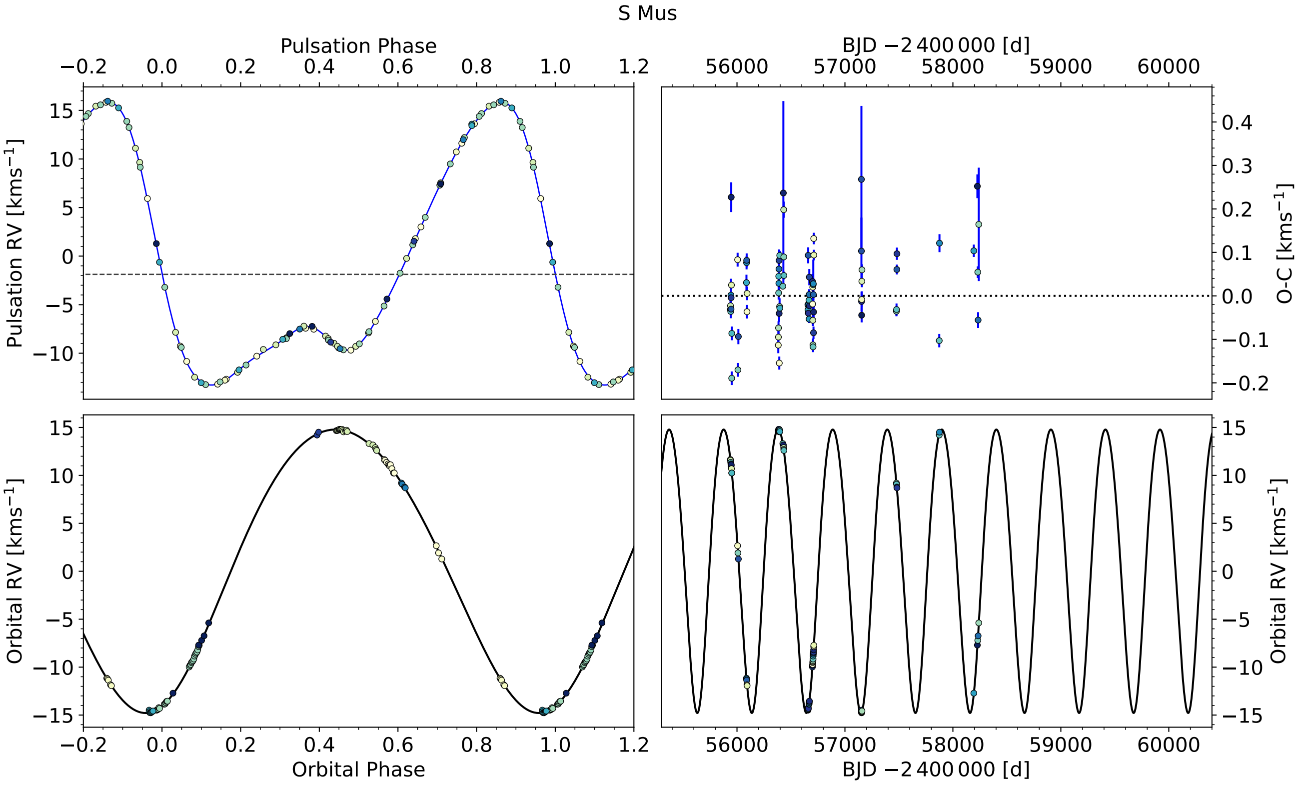

Fig. 16: Pulsational and orbital fit of S Mus. The figure description is the same as Figure 1.

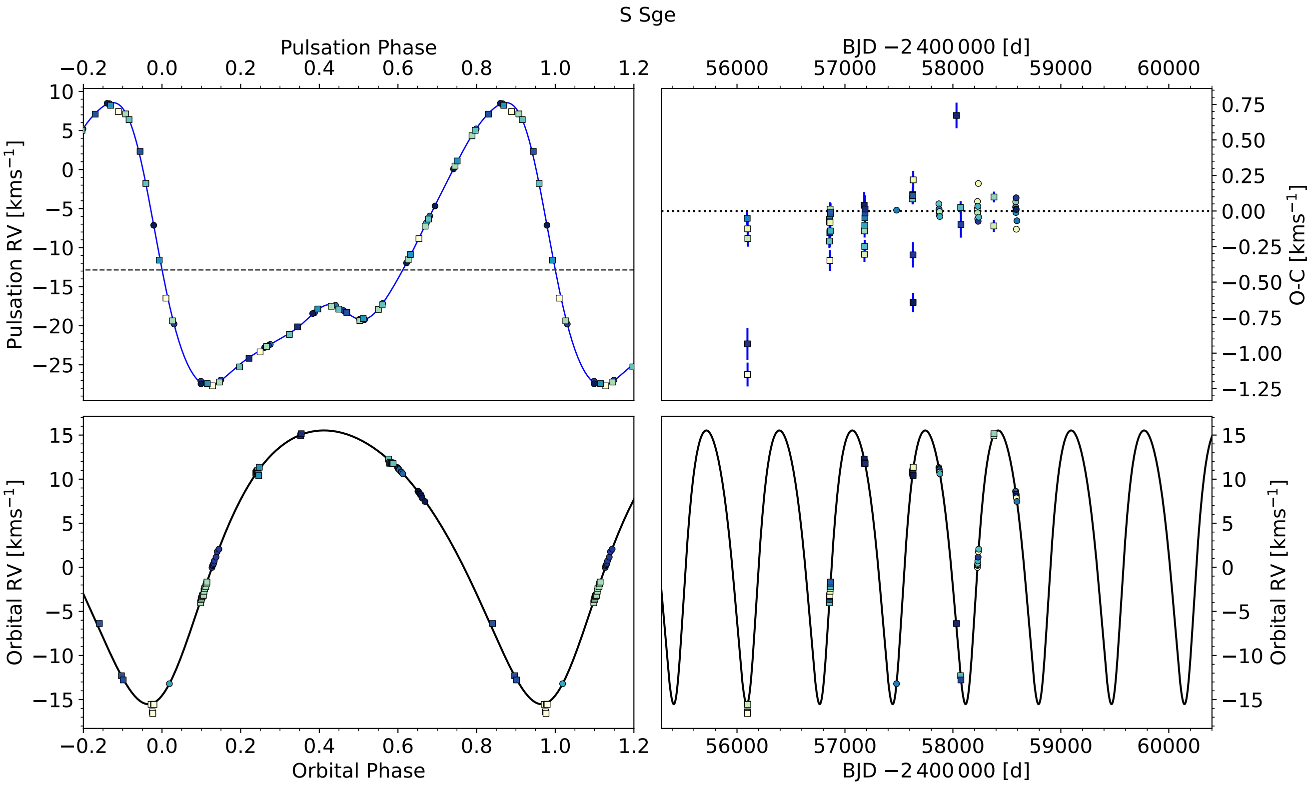

Fig. 17: Pulsational and orbital fit of S Sge. The figure description is the same as Figure 1.

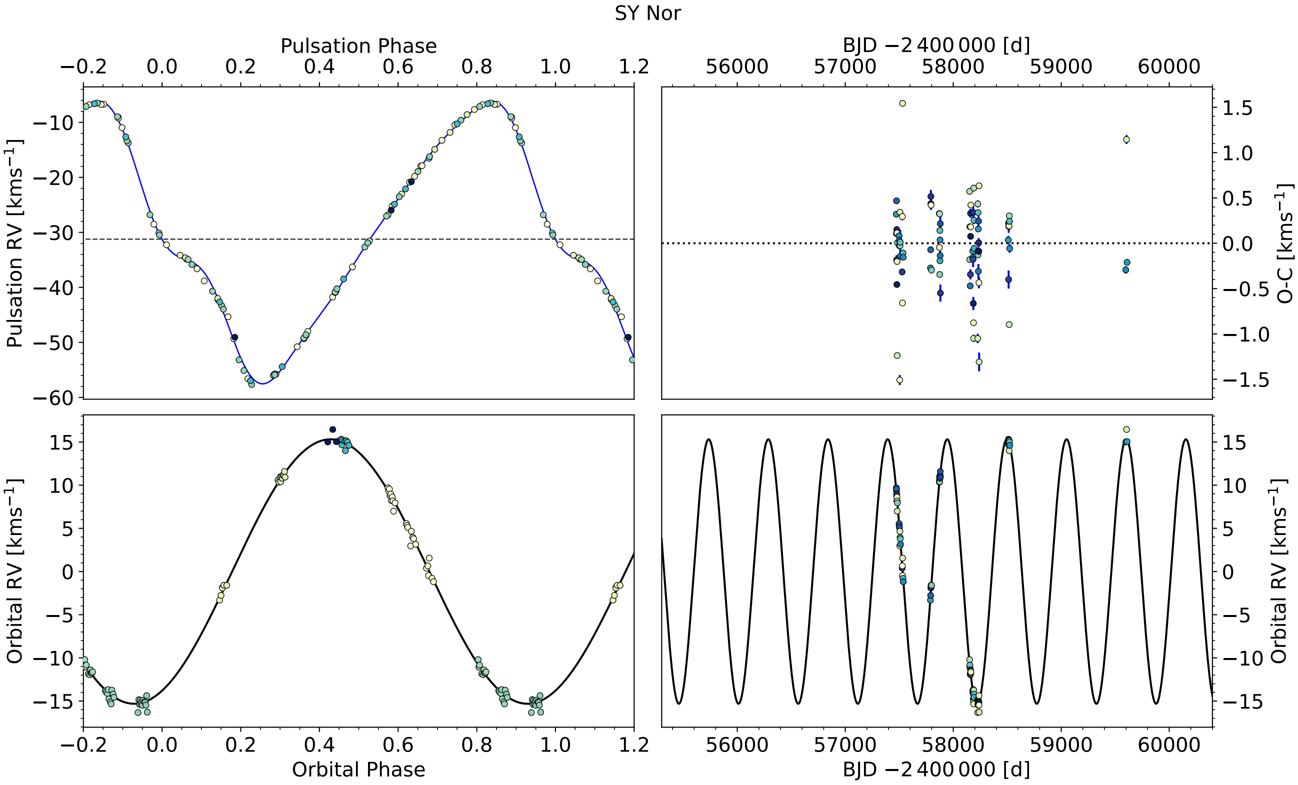

Fig. 18: Pulsational and orbital fit of SY Nor. The figure description is the same as Figure 1.

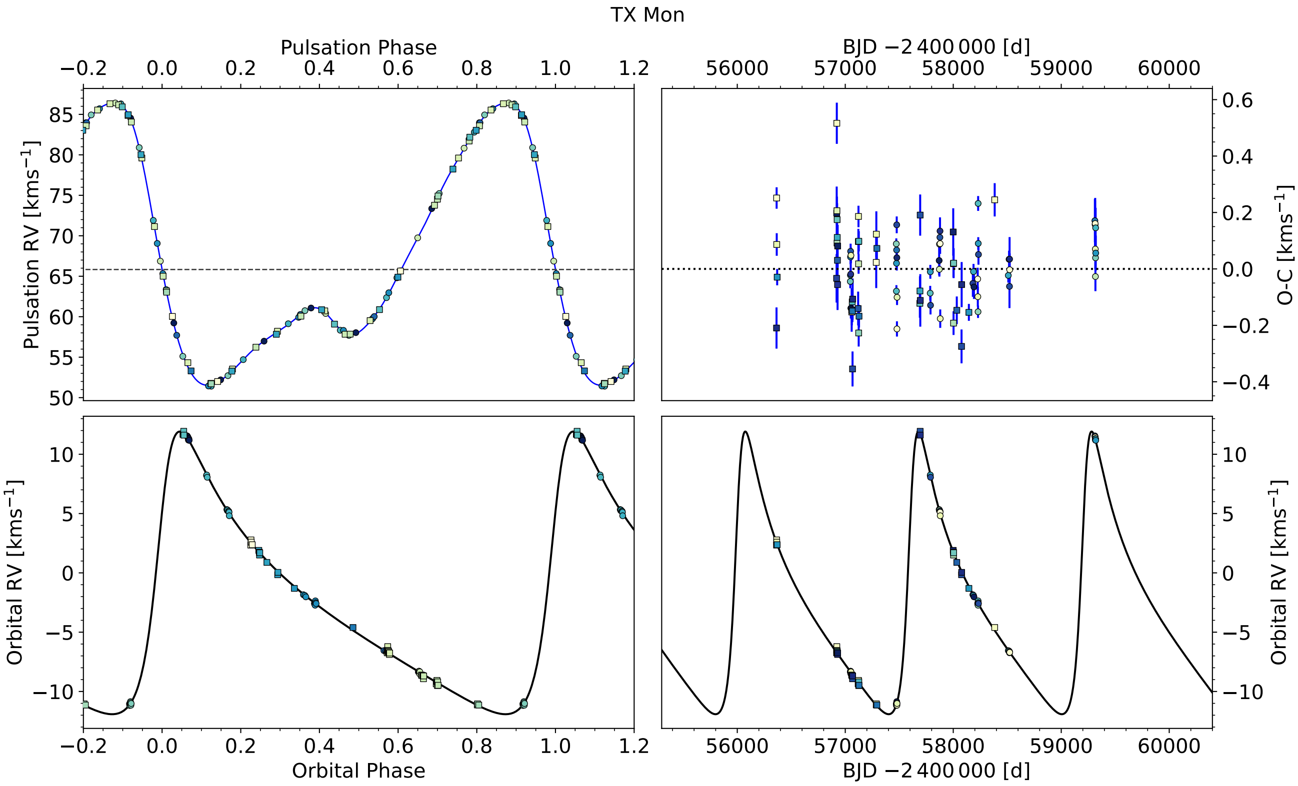

Fig. 19: Pulsational and orbital fit of TX Mon. The figure description is the same as Figure 1.

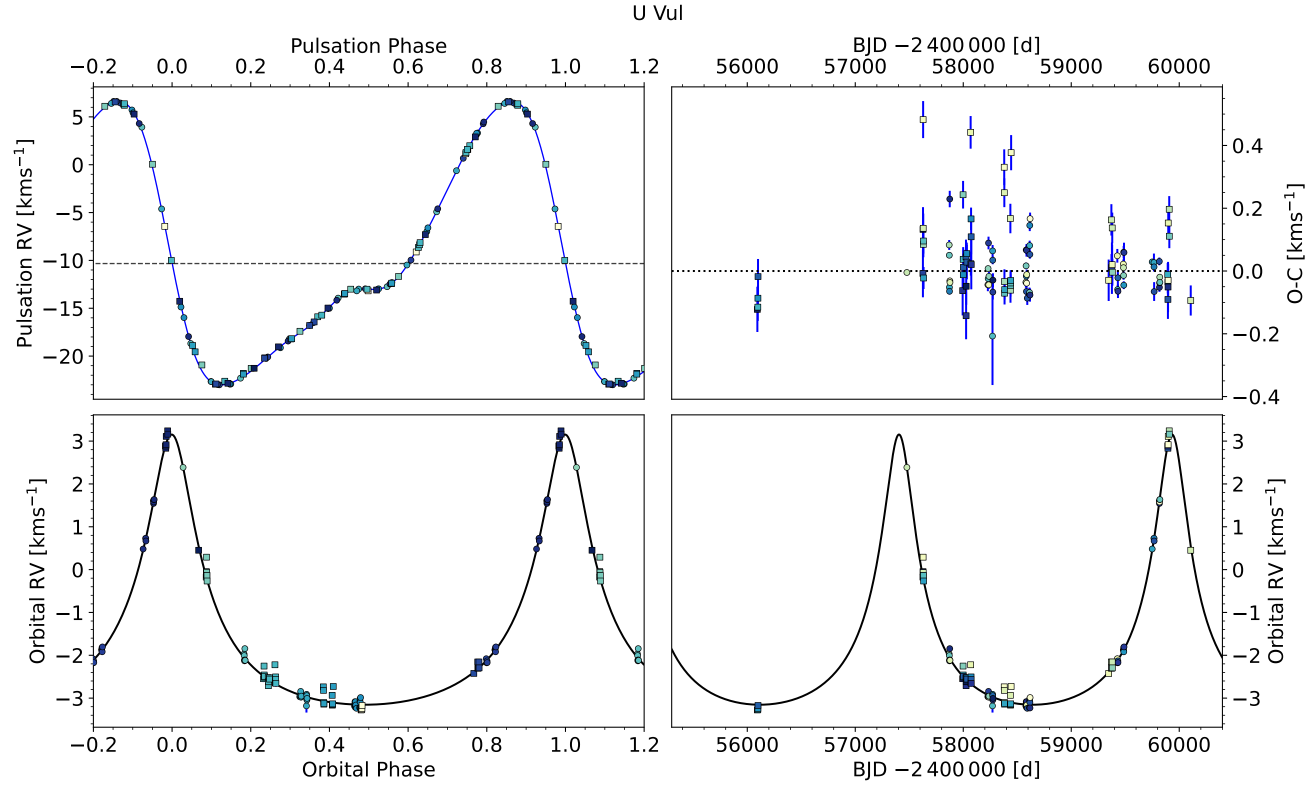

Fig. 20: Pulsational and orbital fit of U Vul. The figure description is the same as Figure 1.

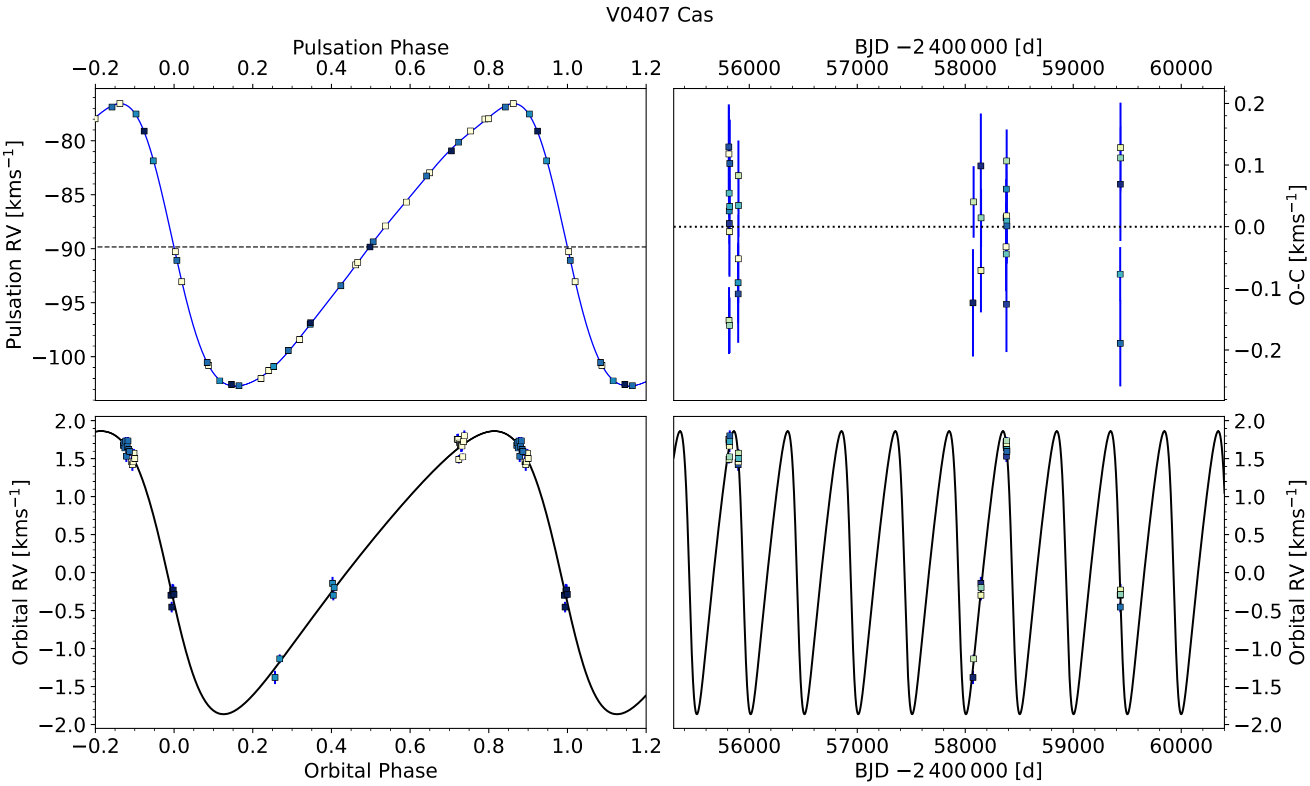

Fig. 21: Pulsational and orbital fit of V0407 Cas. The figure description is the same as Figure 1.

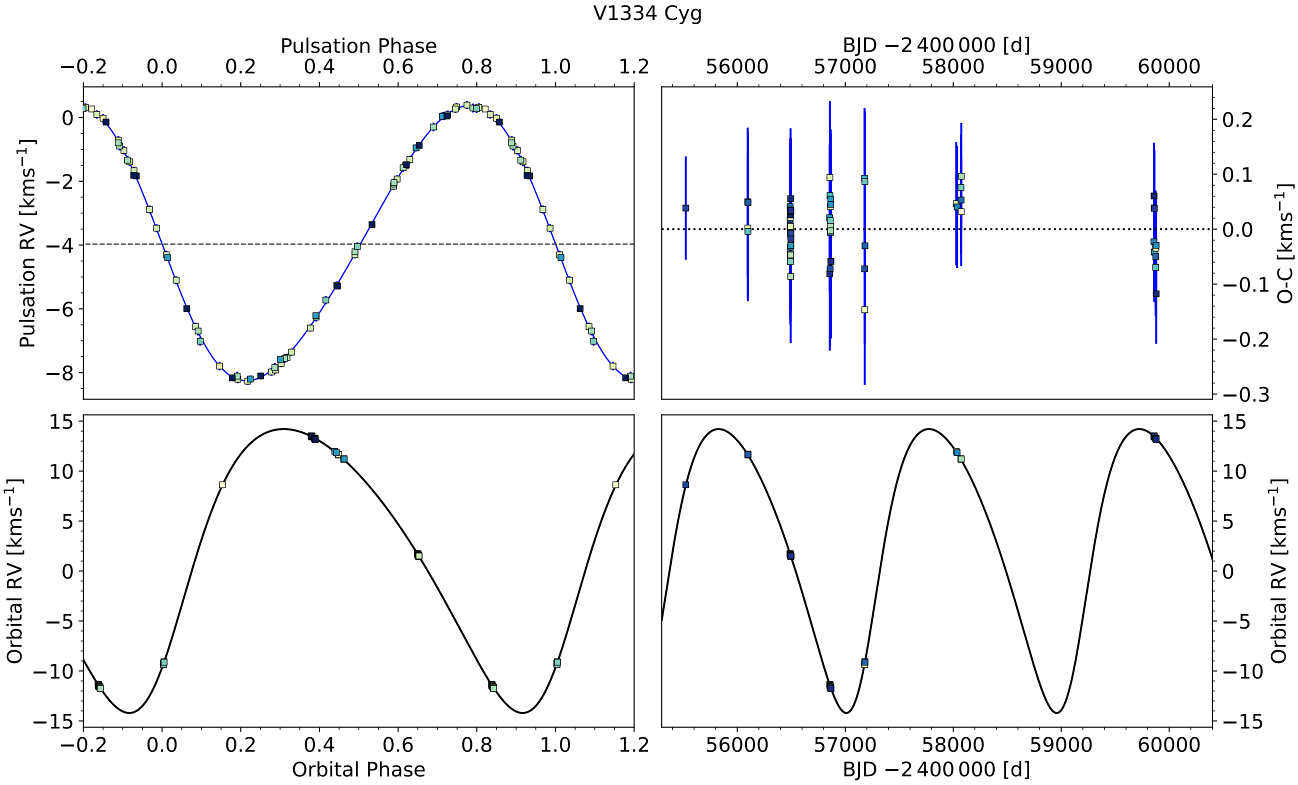

Fig. 22: Pulsational and orbital fit of V1334 Cyg. The figure description is the same as Figure 1.

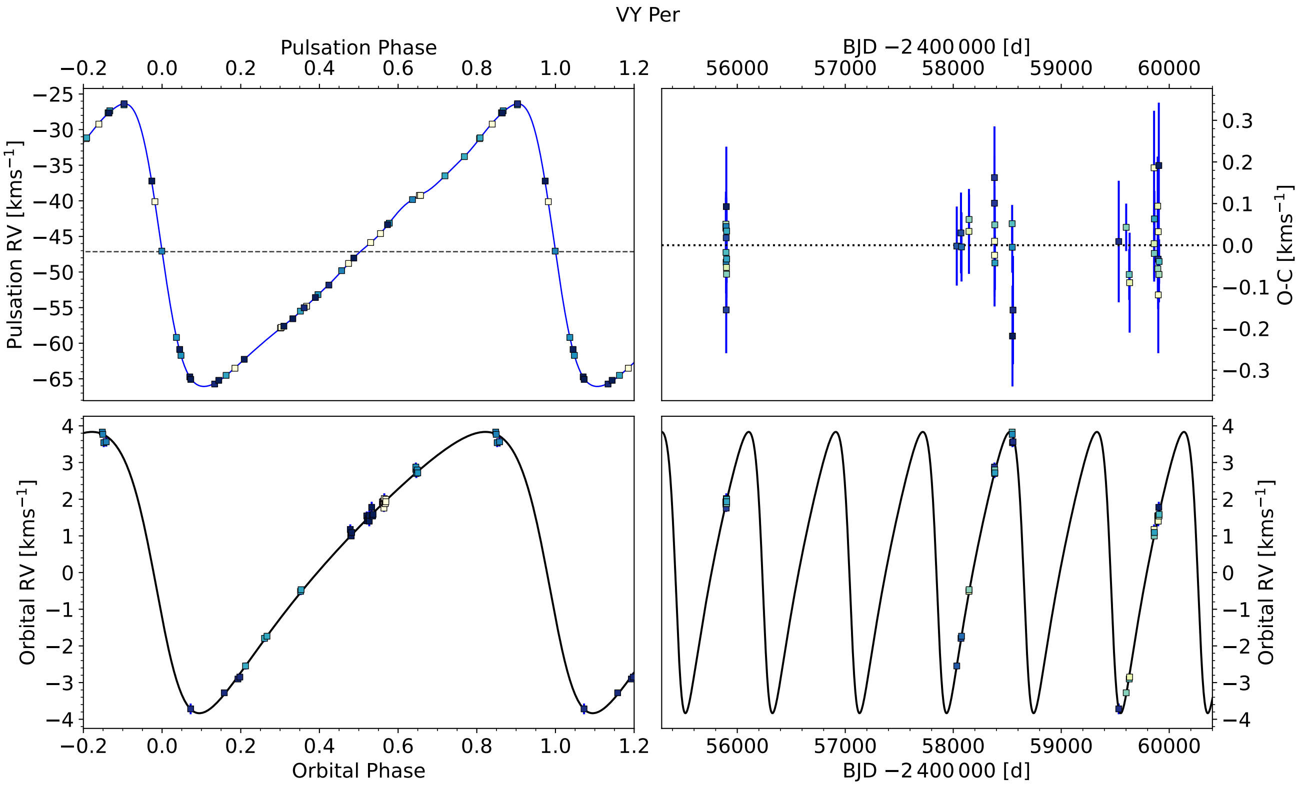

Fig. 23: Pulsational and orbital fit of VY Per. The figure description is the same as Figure 1.

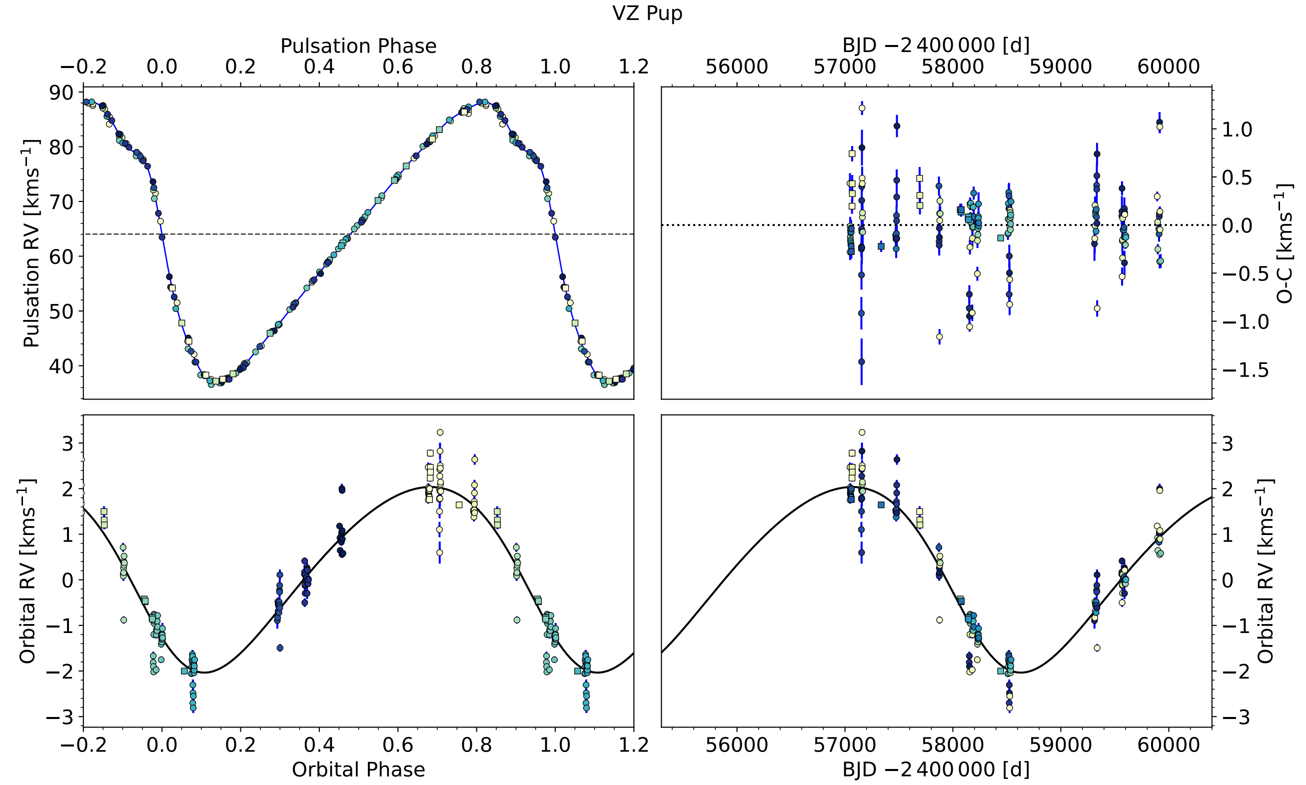

Fig. 24: Pulsational and orbital fit of VZ Pup. The figure description is the same as Figure 1.

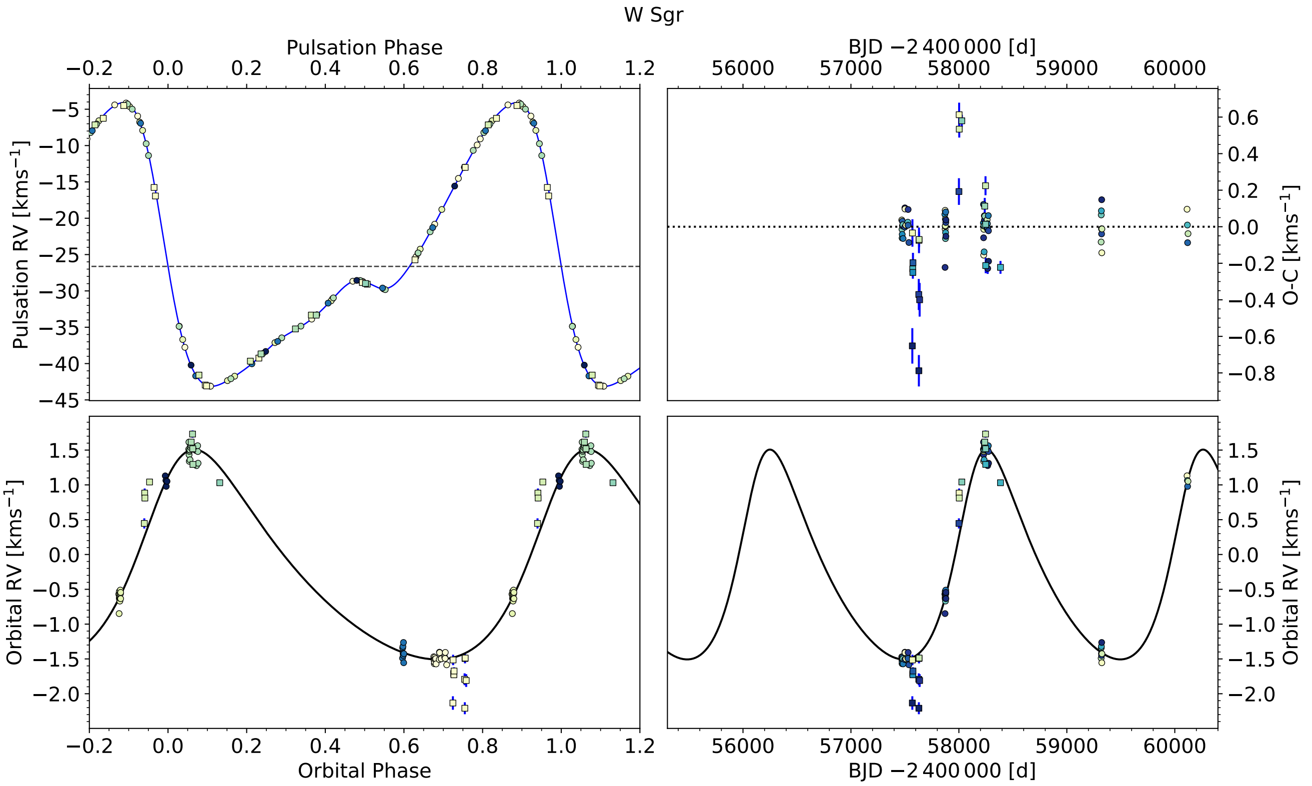

Fig. 25: Pulsational and orbital fit of W Sgr. The figure description is the same as Figure 1. The bottom right panel suggests that the orbit of W Sgr could be more eccentric than the best fit model obtained here.

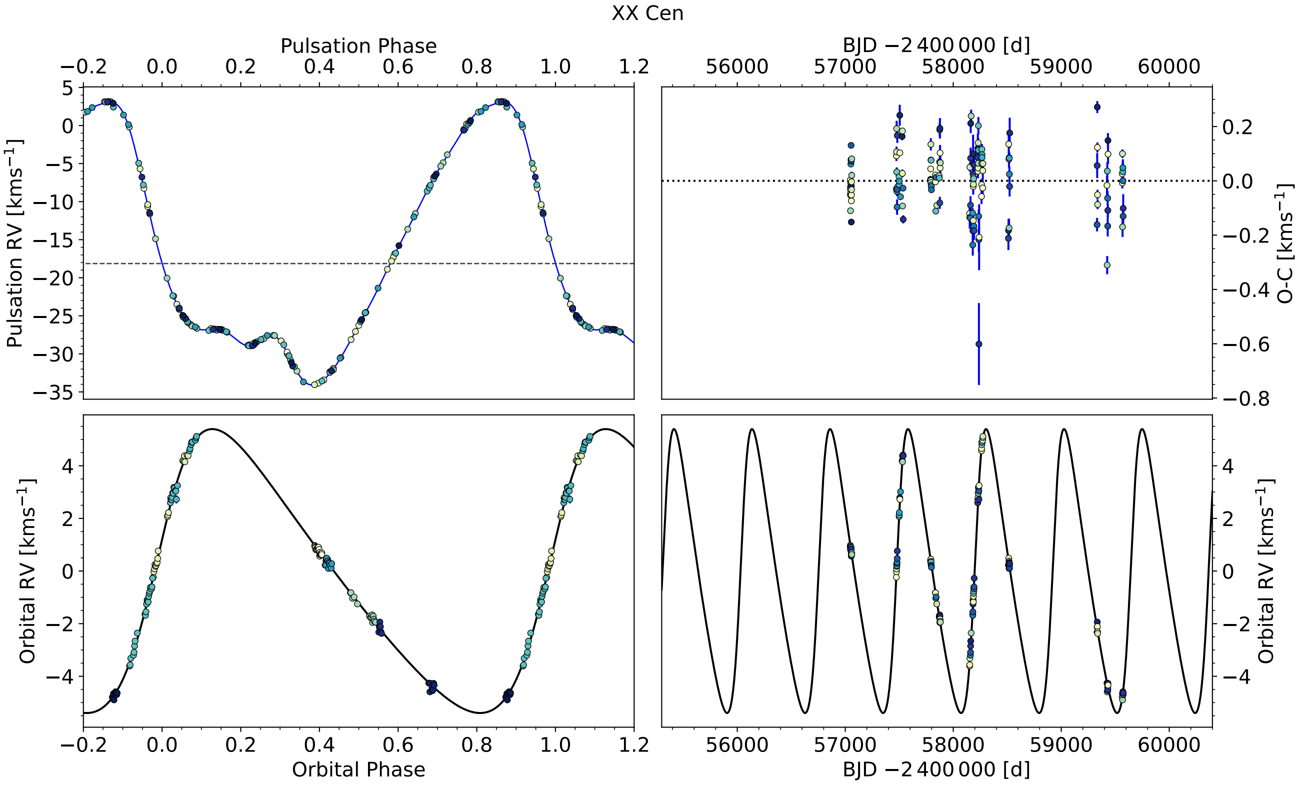

Fig. 26: Pulsational and orbital fit of XX Cen. The figure description is the same as Figure 1.

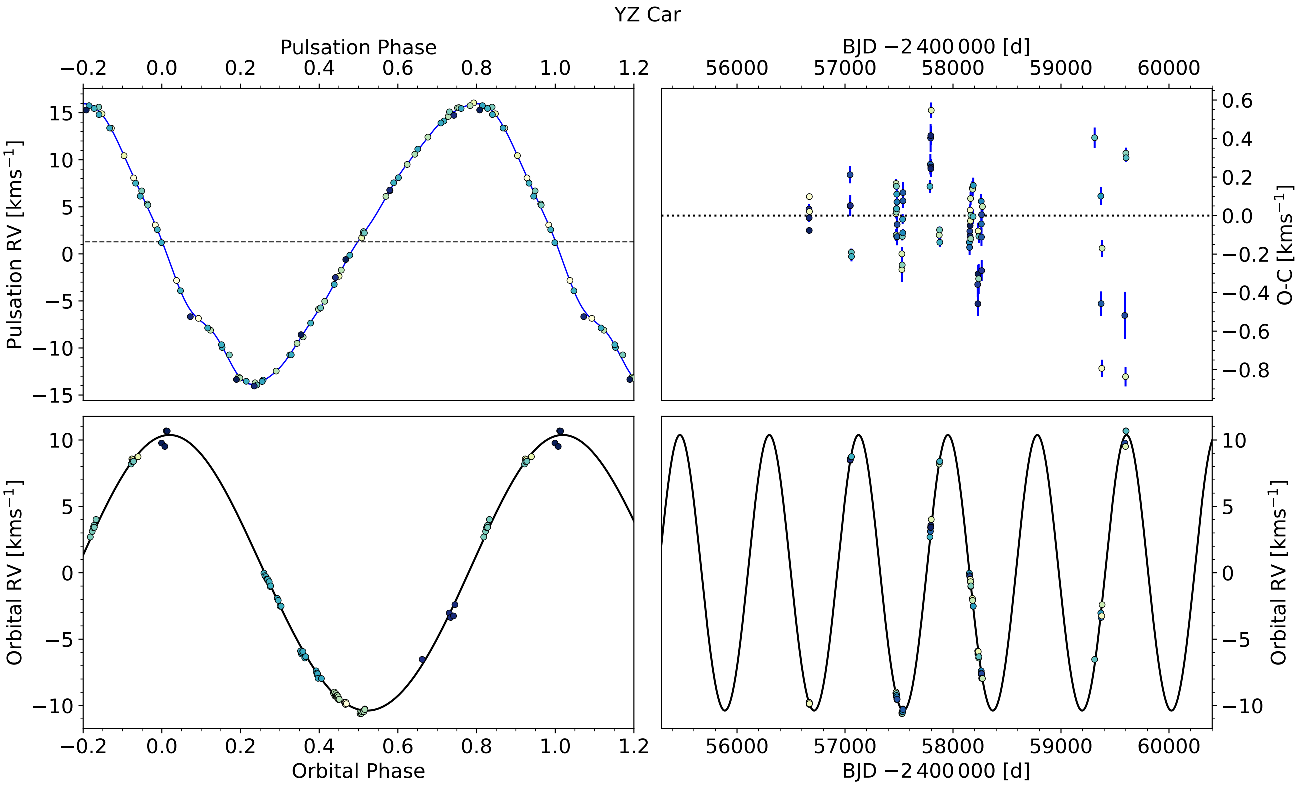

Fig. 27: Pulsational and orbital fit of YZ Car. The figure description is the same as Figure 1.

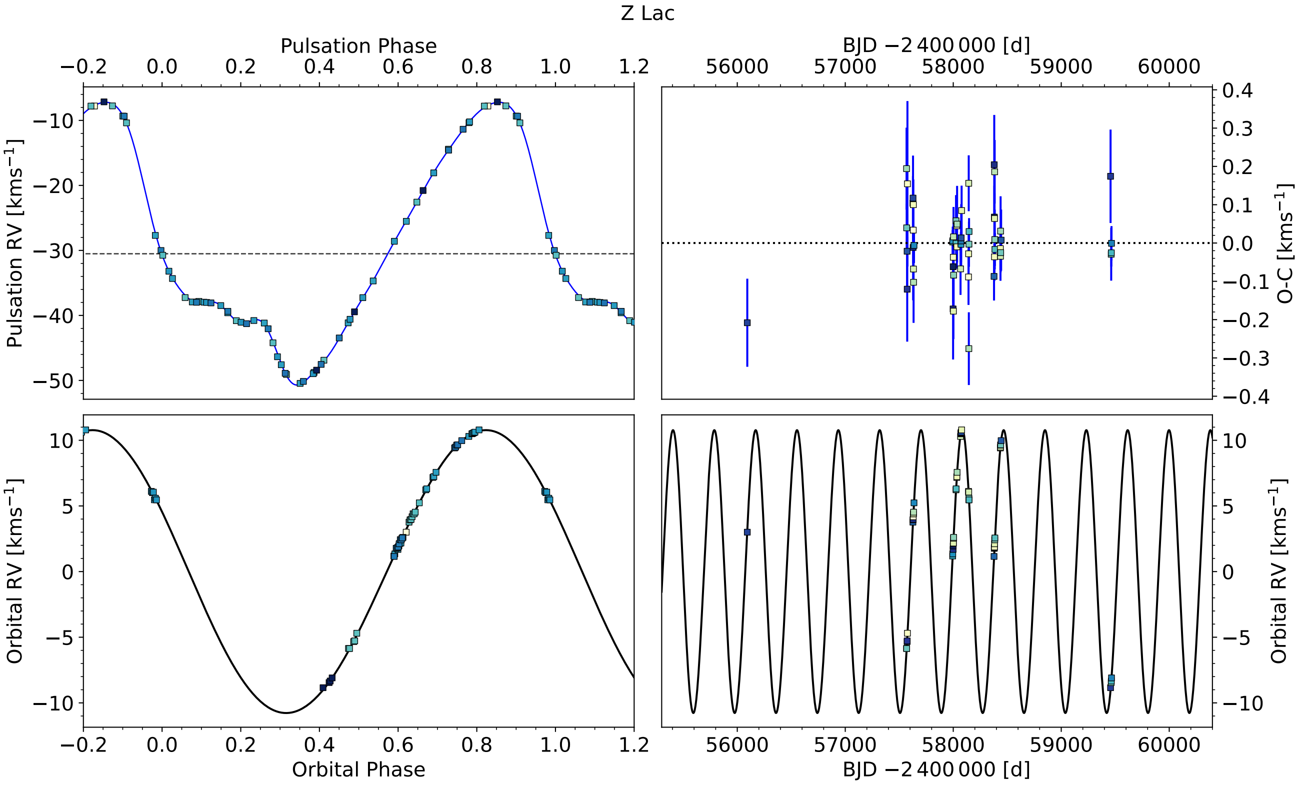

Fig. 28: Pulsational and orbital fit of Z Lac. The figure description is the same as Figure 1.

2.2. Orbits from VELOCE and literature data (V+L)

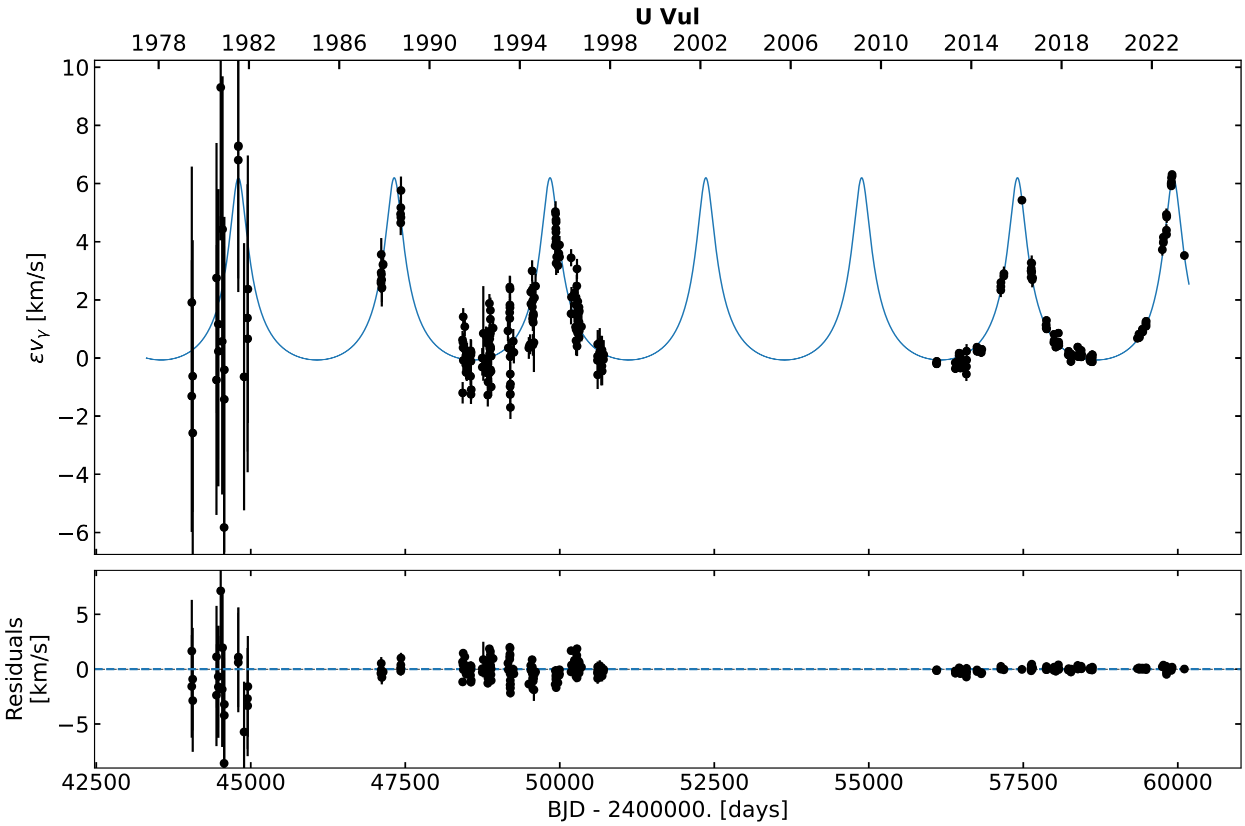

Fig. 29: Orbit of U Vul determined by fitting v_γ epoch residuals of literature and VELOCE data.

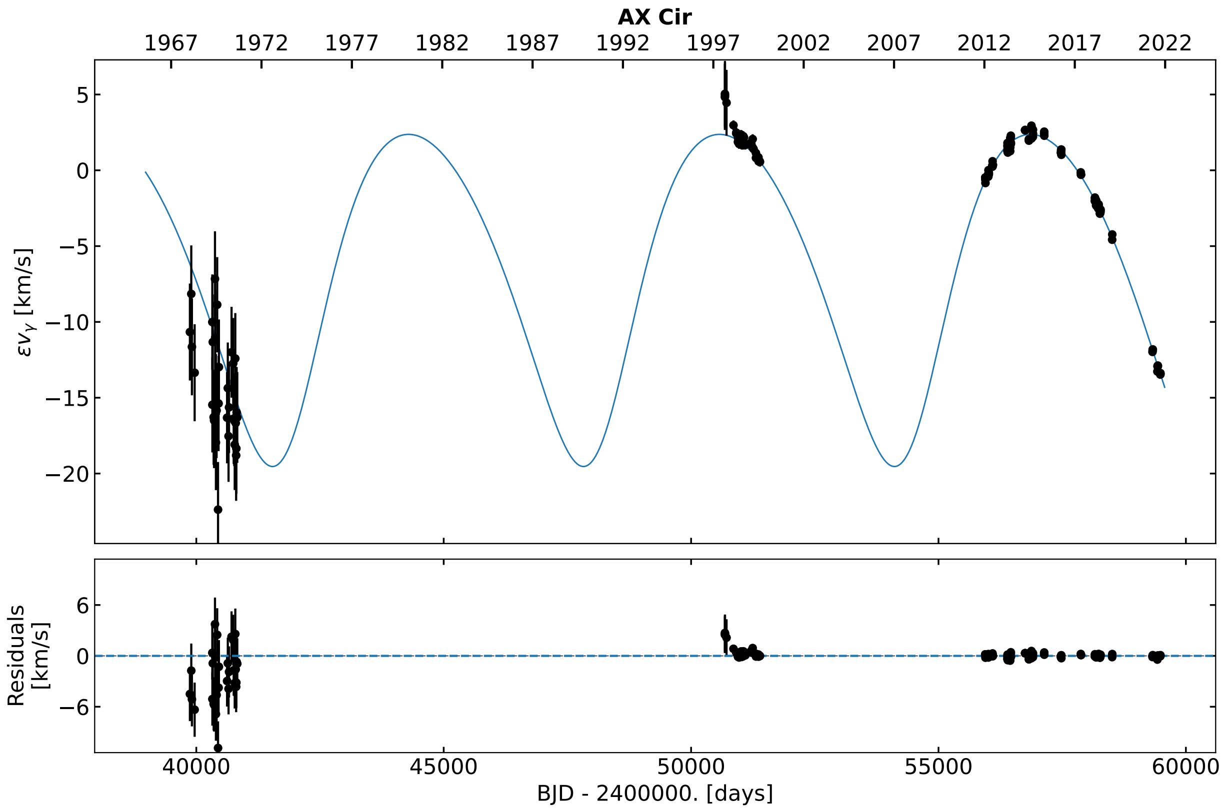

Fig. 30: V_γ residuals Orbit fitting for AX Cir.

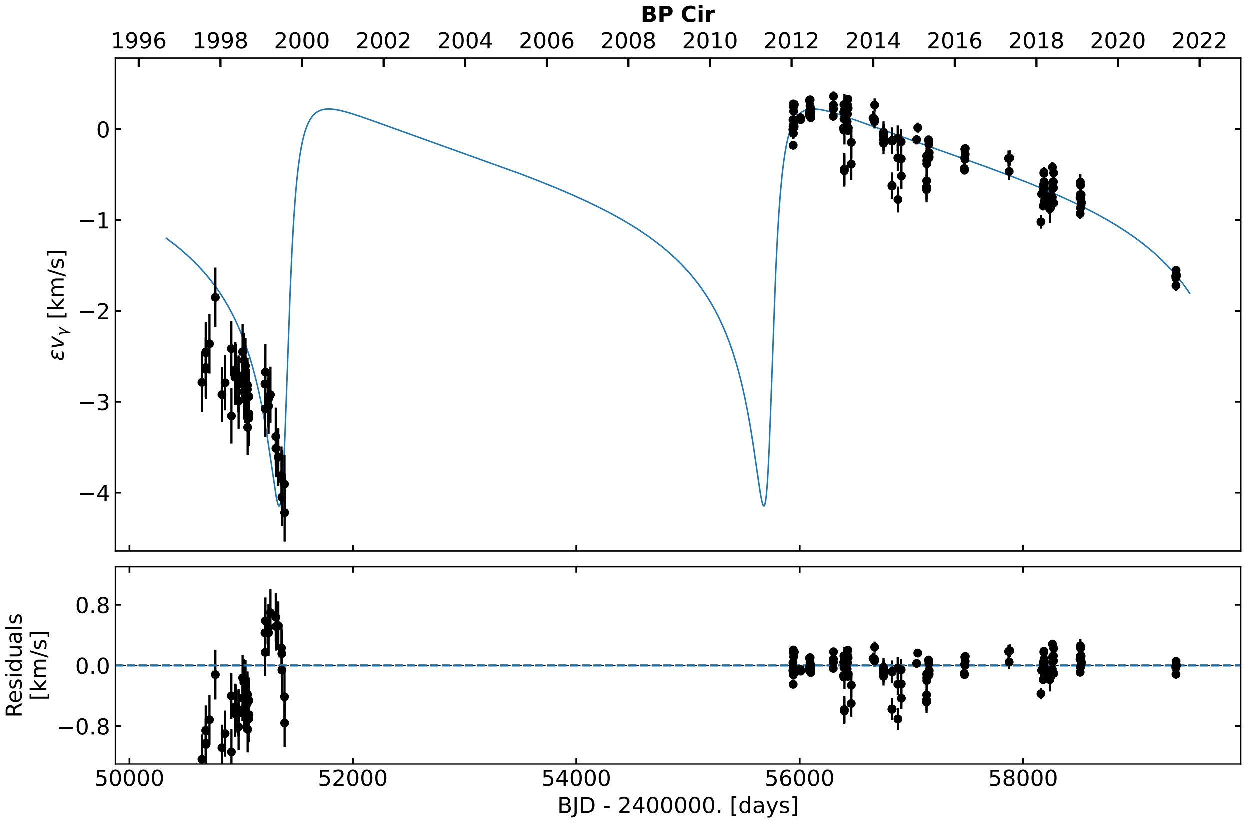

Fig. 31: V_{γ} residuals Orbit fitting for BP Cir.

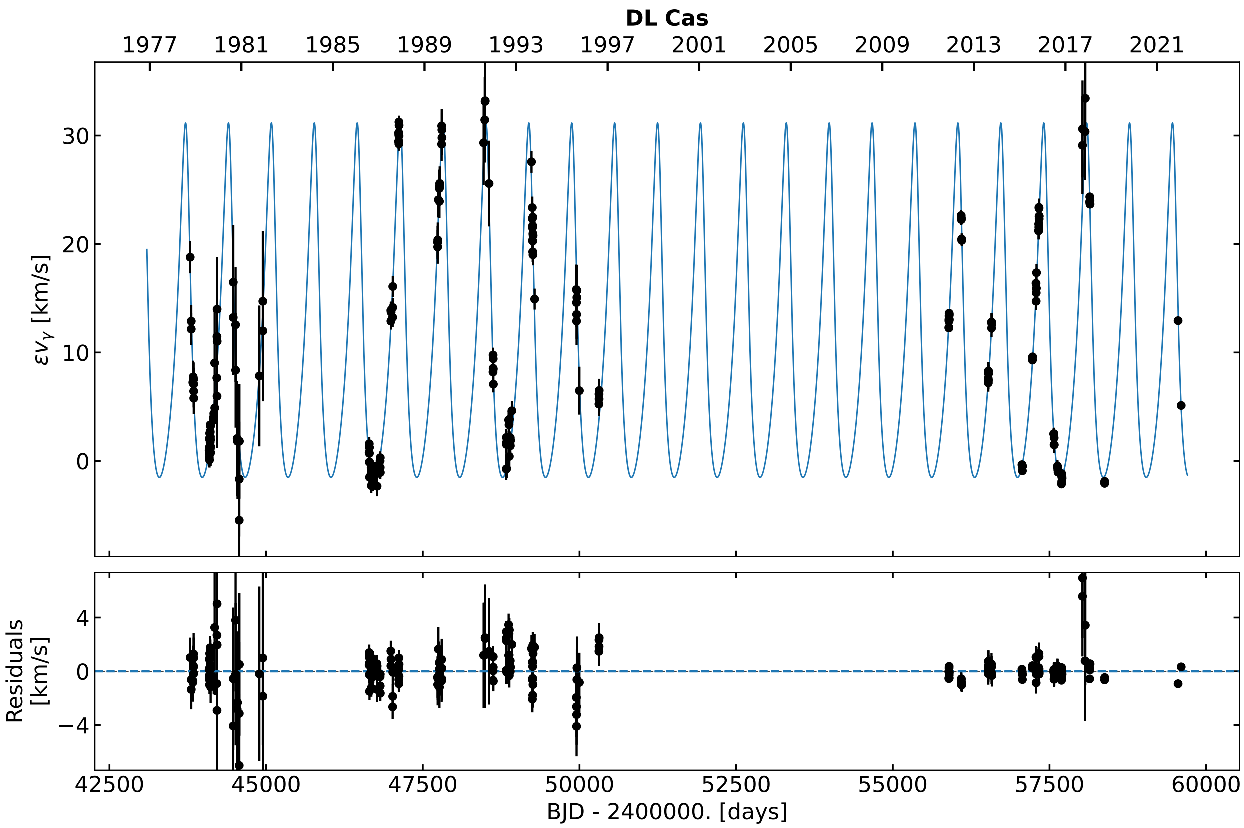

Fig. 32: V_{γ} residuals Orbit fitting for DL Cas.

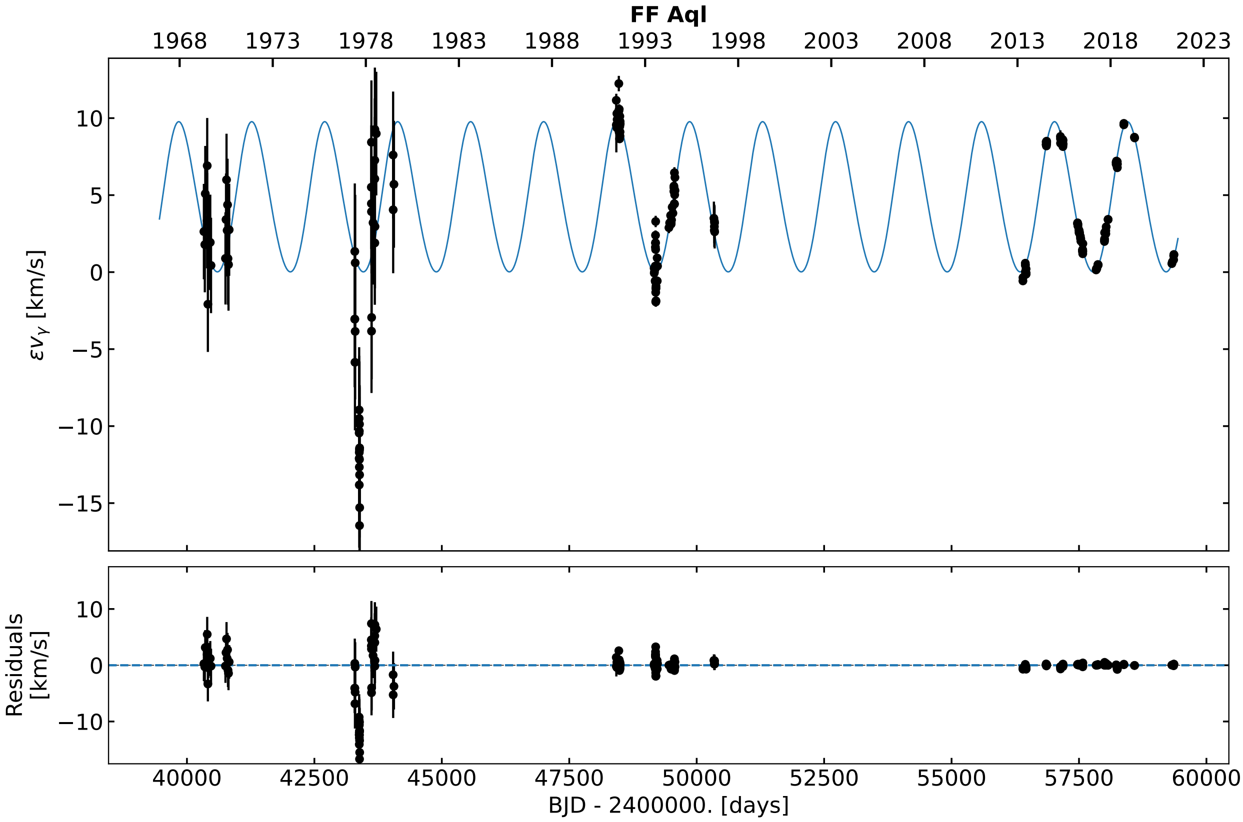

Fig. 33: V_γ residuals Orbit fitting for FF Aql.

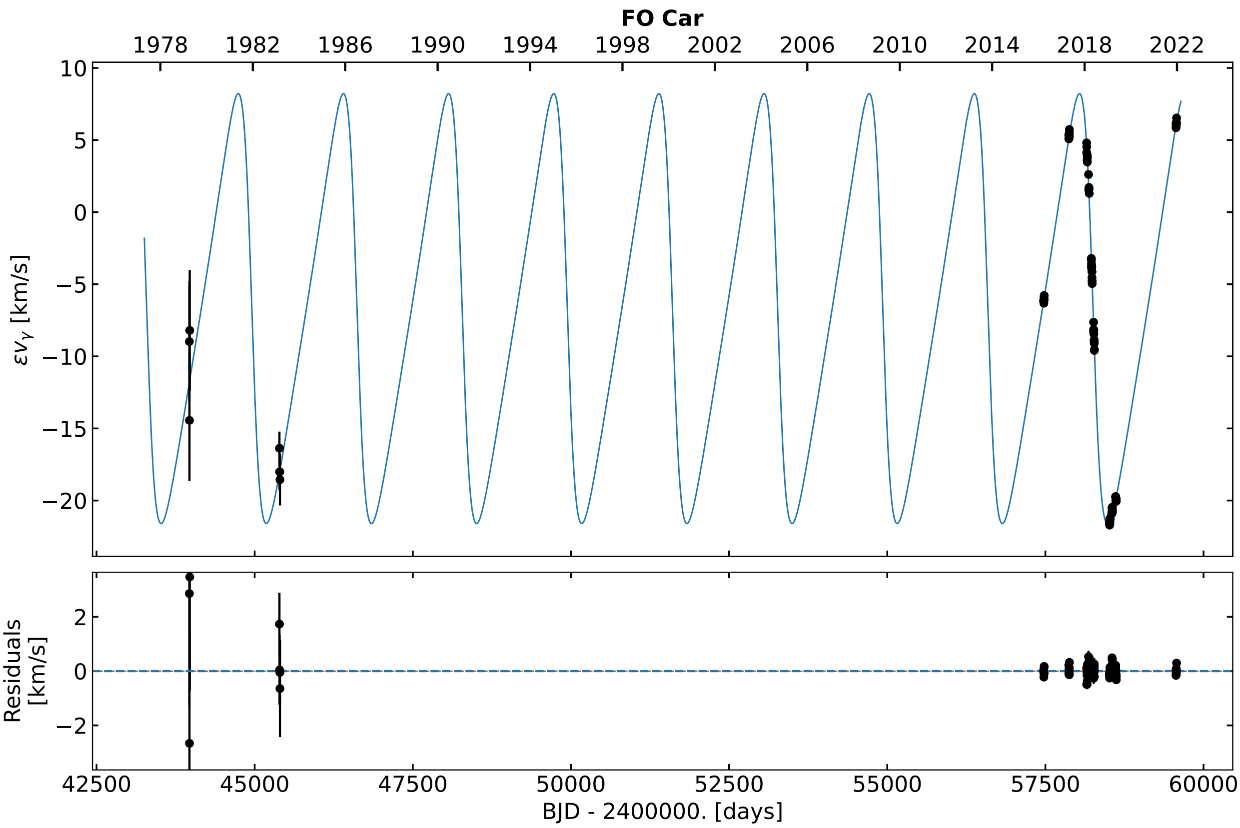

Fig. 34: V_γ residuals Orbit fitting for FO Car.

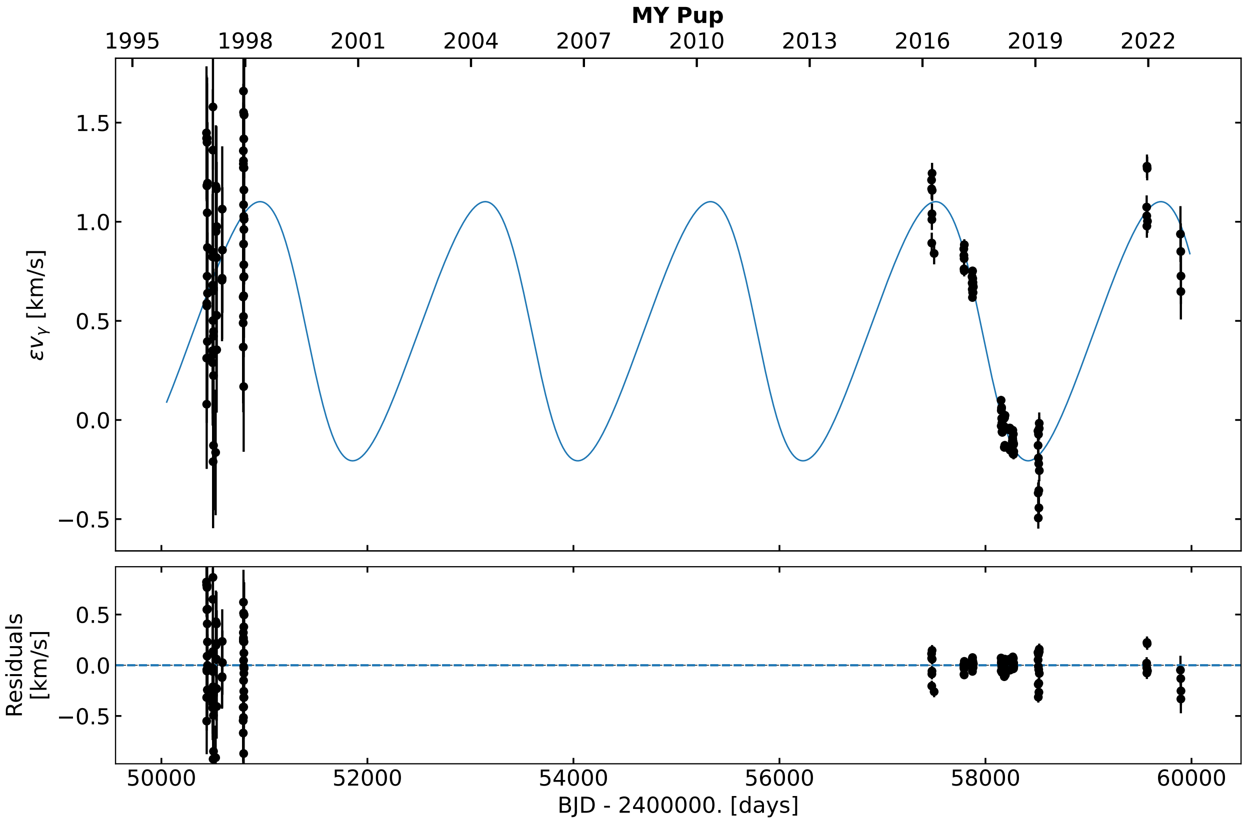

Fig. 35: V_{γ} residuals Orbit fitting for MY Pup.

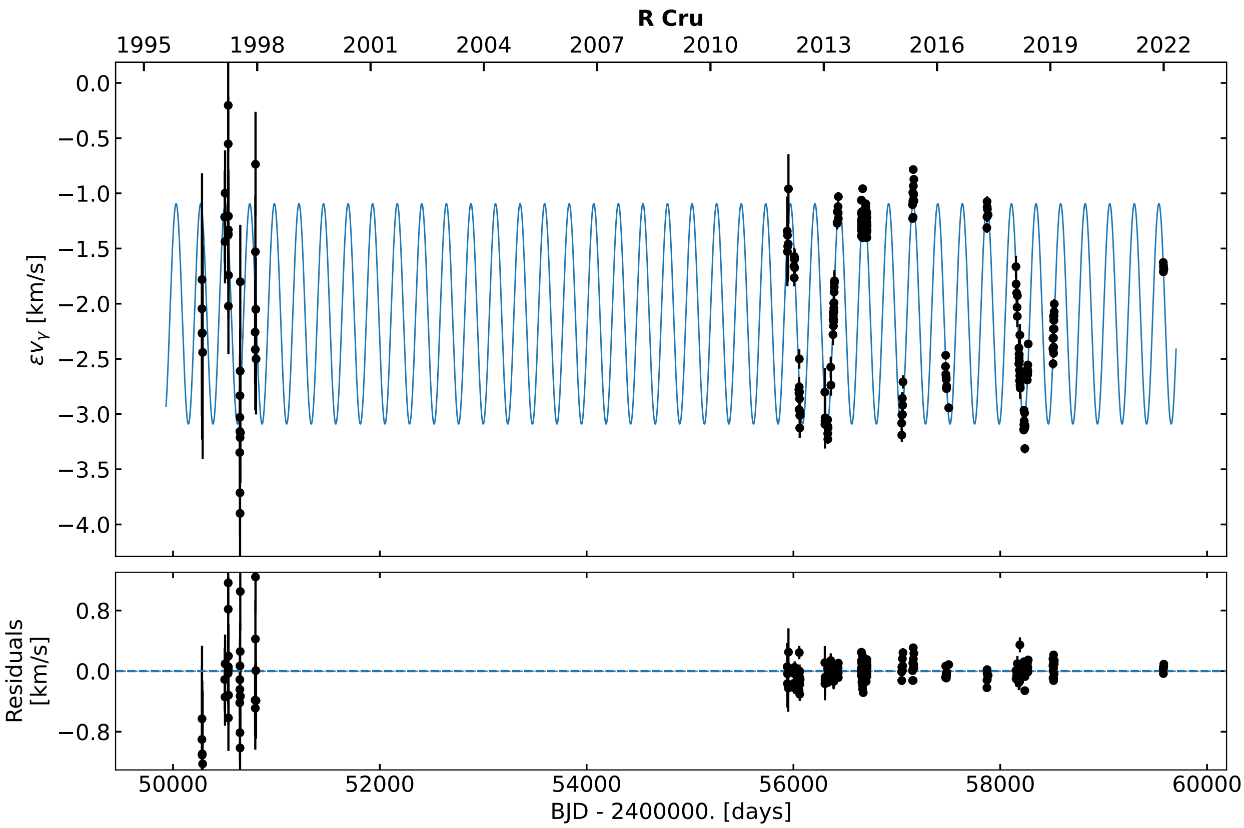

Fig. 36: V_{γ} residuals Orbit fitting for R Cru.

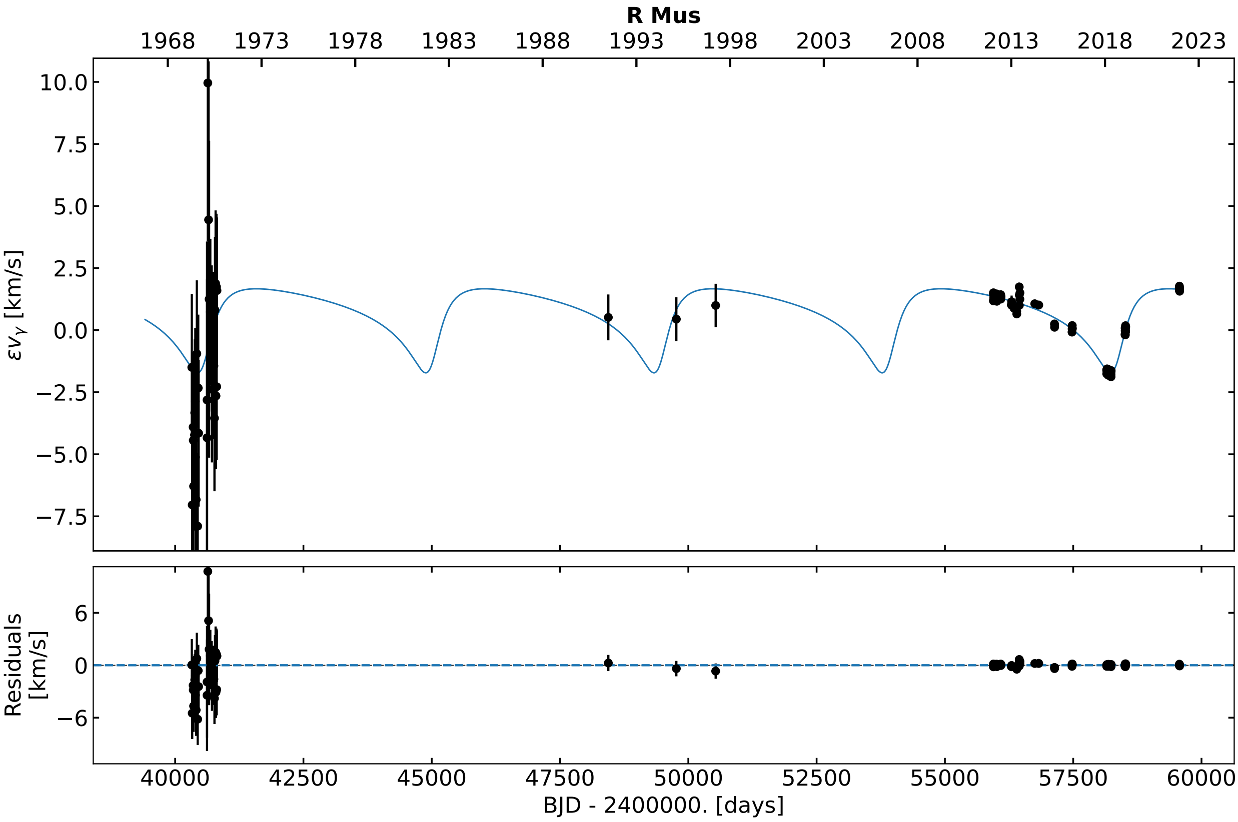

Fig. 37: V_γ residuals Orbit fitting for R Mus.

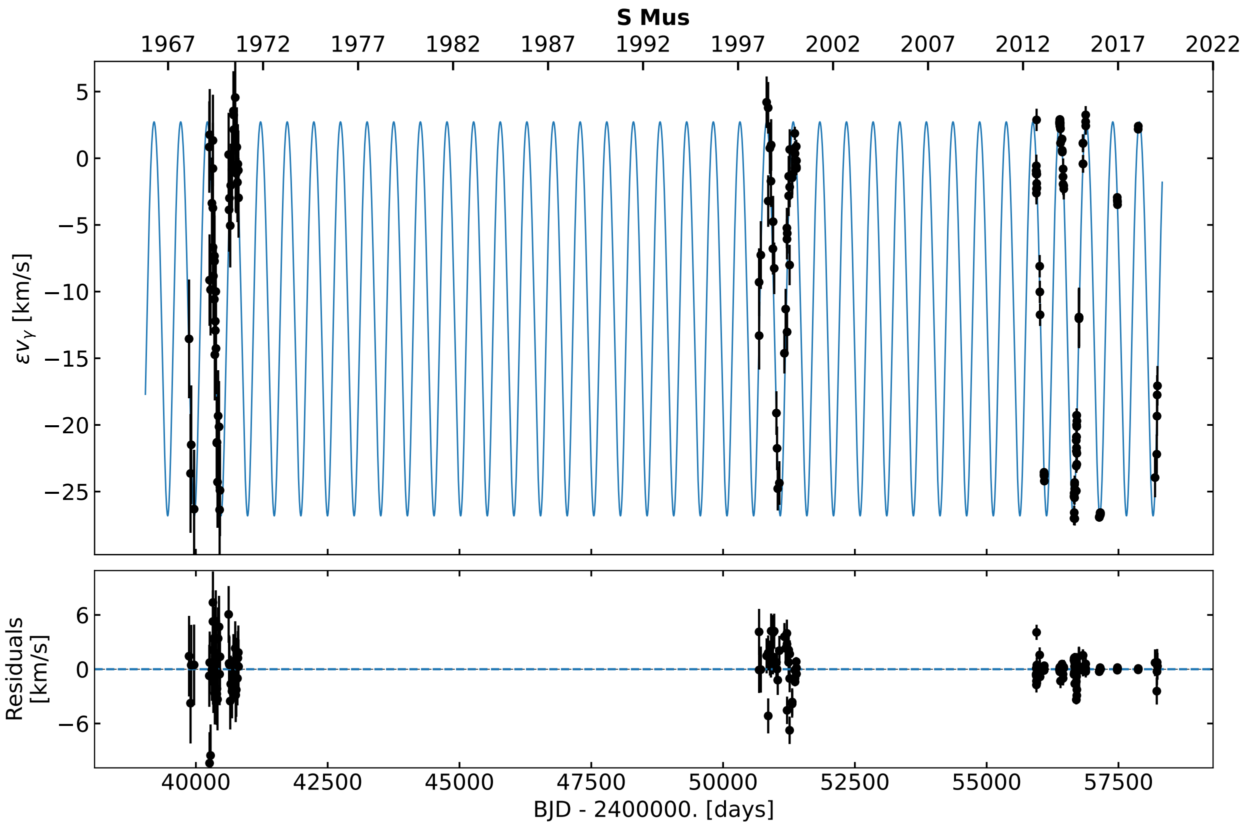

Fig. 38: V_γ residuals Orbit fitting for S Mus.

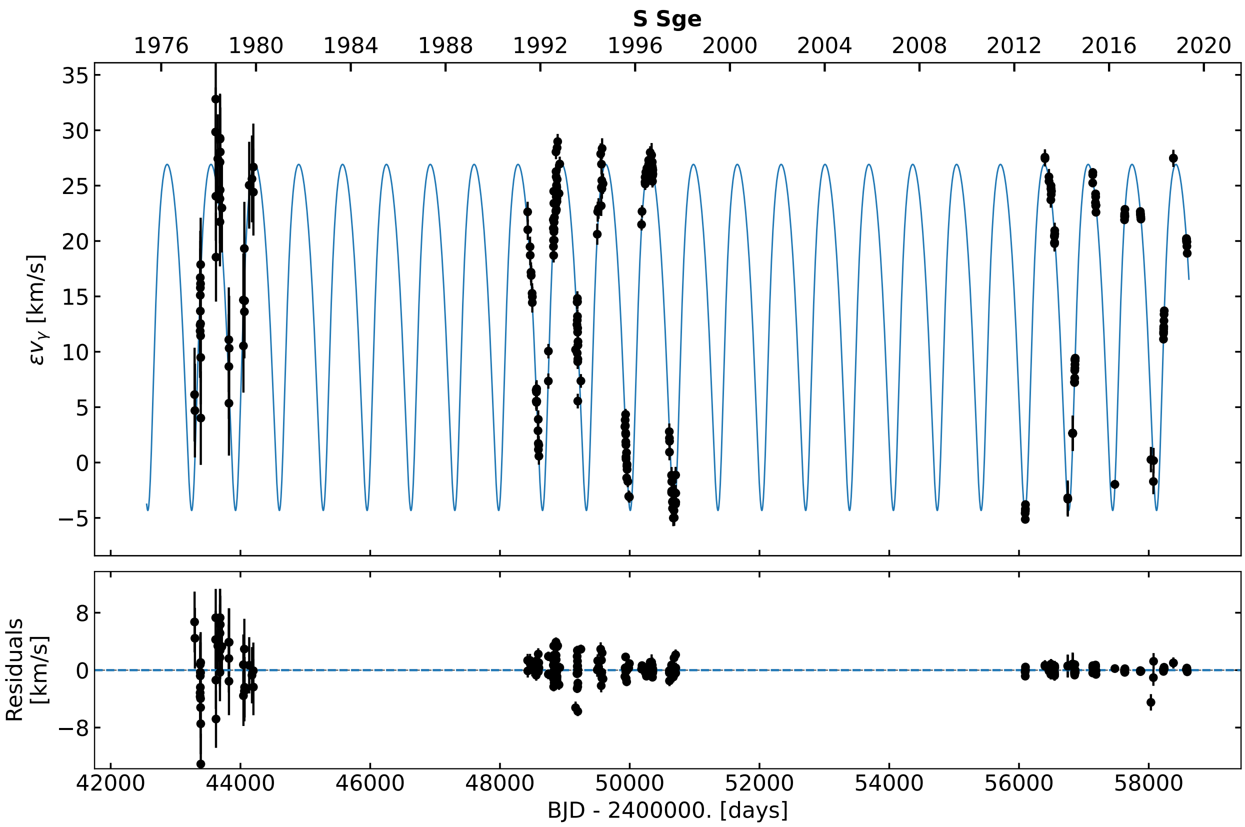

Fig. 39: V_γ residuals Orbit fitting for S Sge.

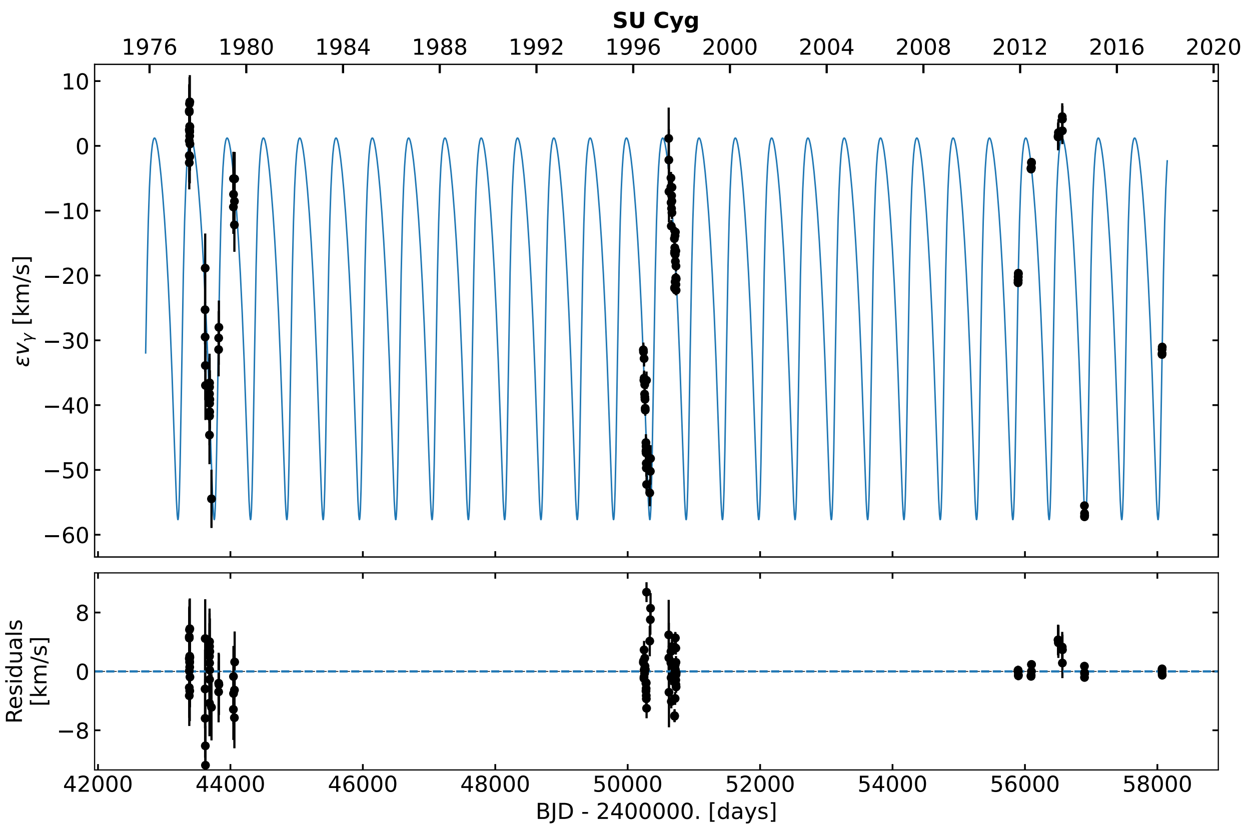

Fig. 40: V_γ residuals Orbit fitting for SU Cyg.

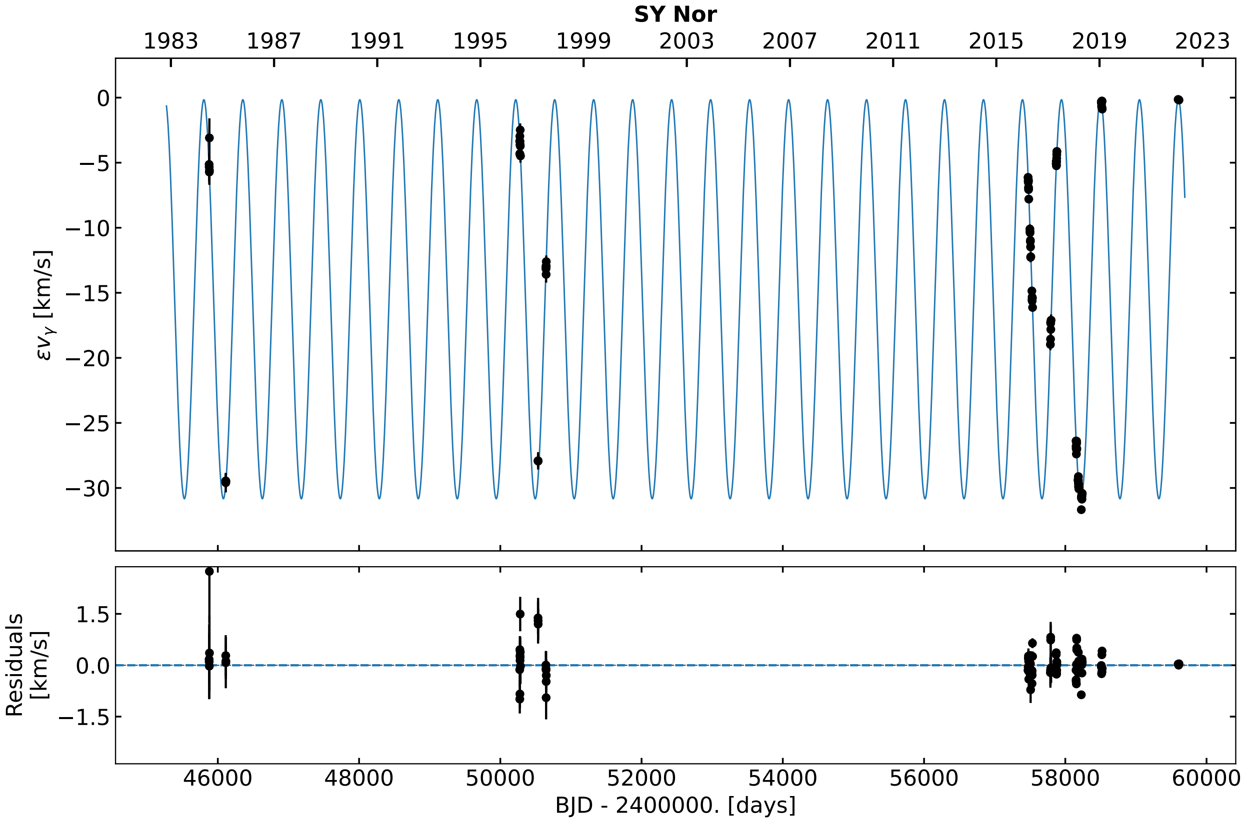

Fig. 41: V_γ residuals Orbit fitting for SY Nor.

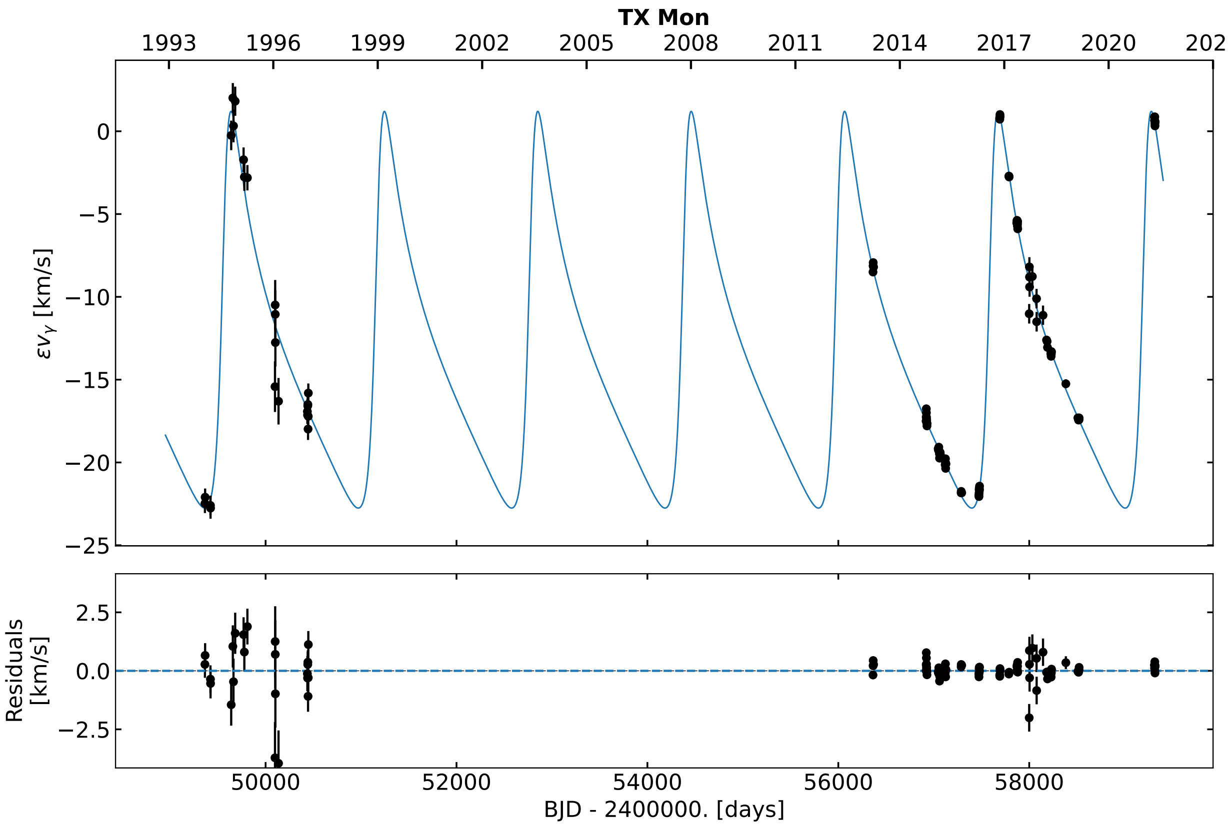

Fig. 42: V_γ residuals Orbit fitting for TX Mon.

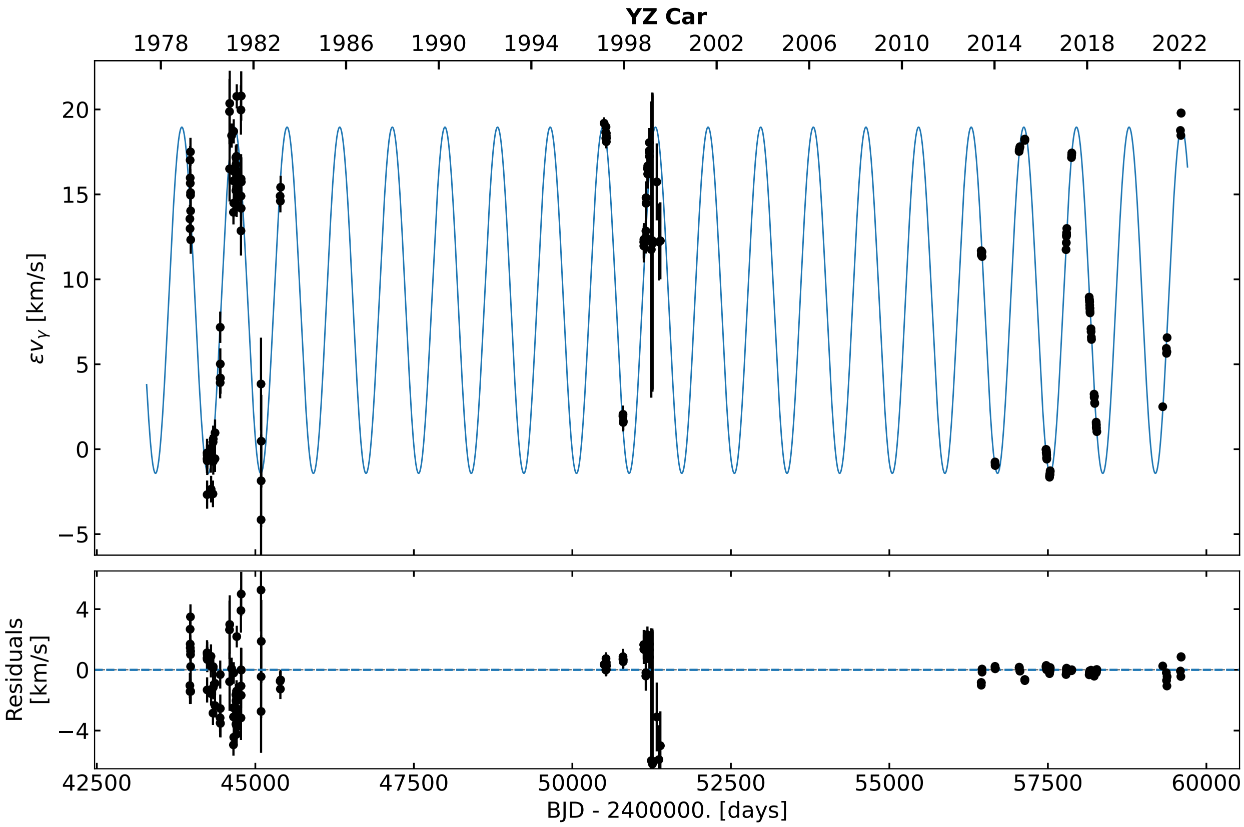

Fig. 43: V_γ residuals Orbit fitting for YZ Car.

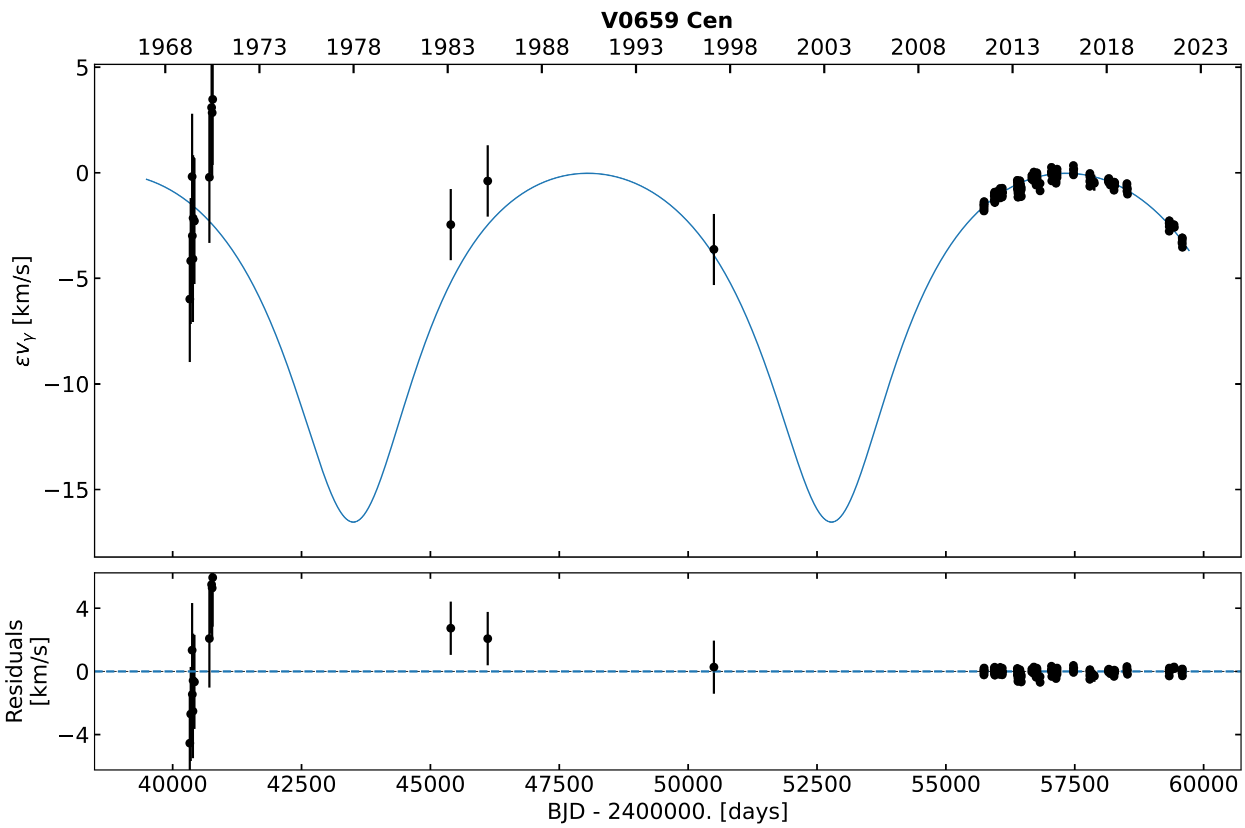

Fig. 44: V_γ residuals Orbit fitting for V0659 Cen.

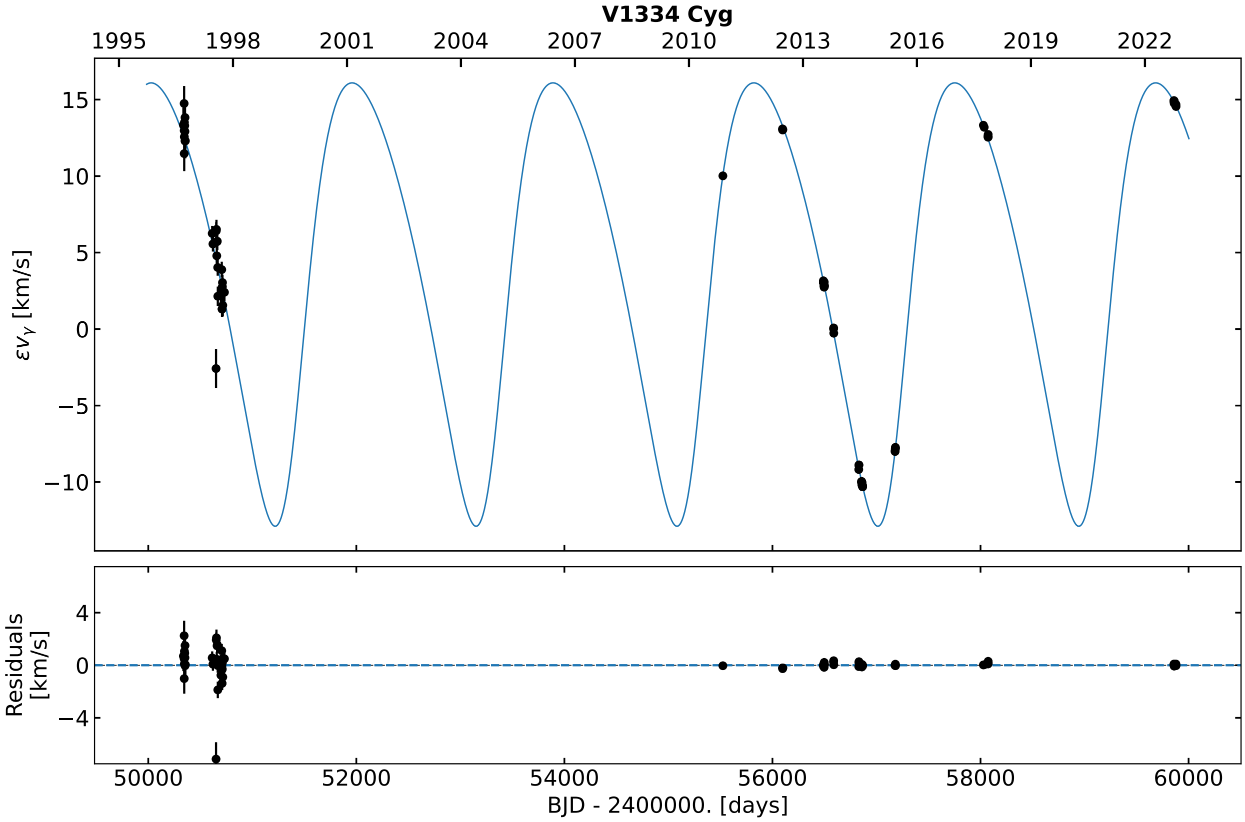

Fig. 45: V_γ residuals Orbit fitting for V1334 Cyg.

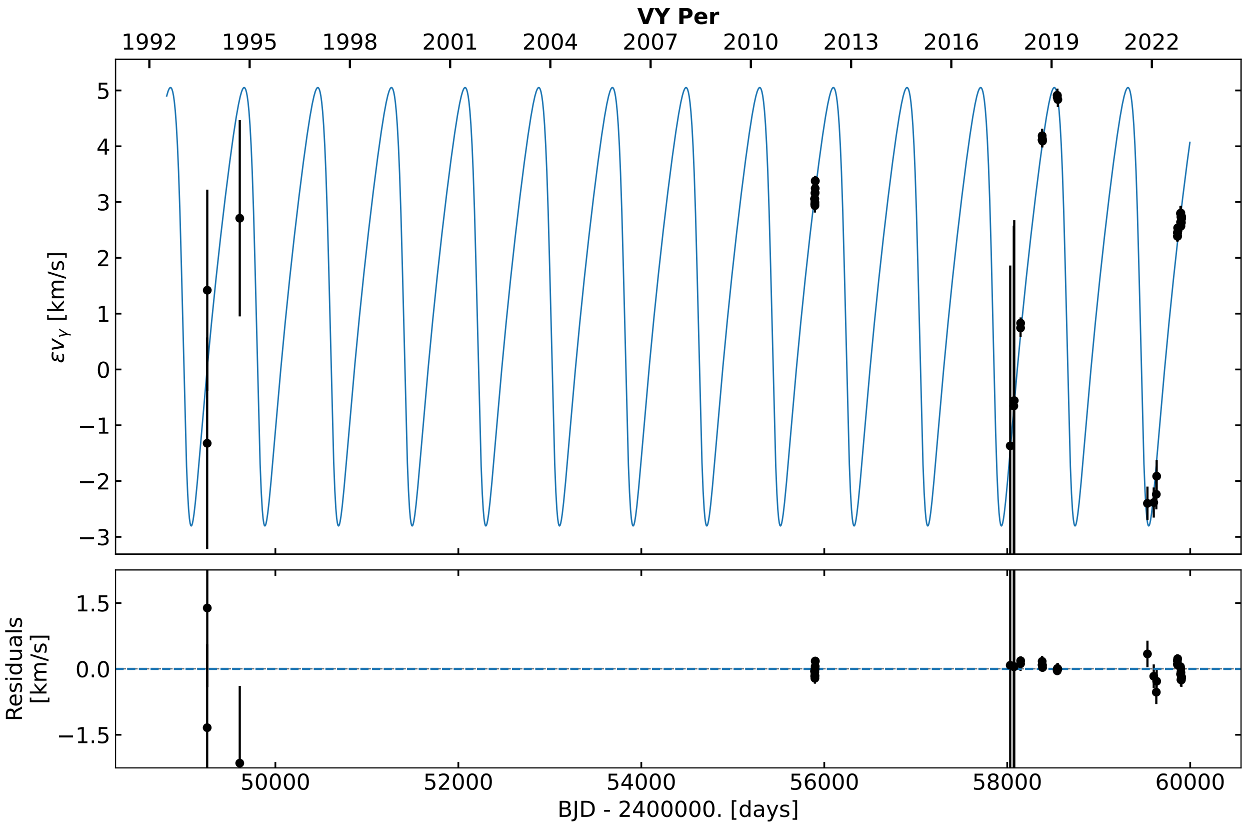

Fig. 46: V_γ residuals Orbit fitting for VY Per.

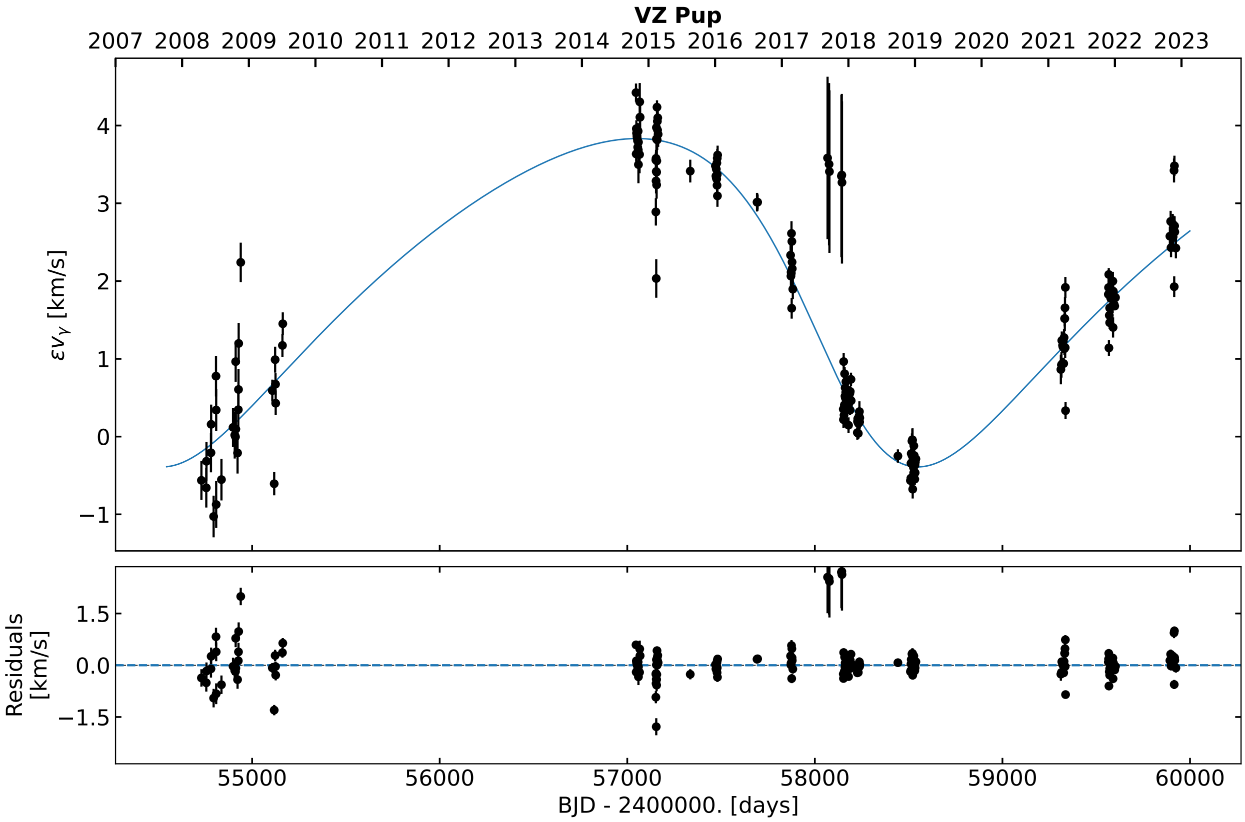

Fig. 47: V_γ residuals Orbit fitting for VZ Pup.

3. Incompletely sampled orbits modeled as polynomial trends

Sample stars with incompletely sampled orbits were fitted using a combined Fourier series plus polynomial trend In Table 4, we present the related quantities, the polynomial fitting method is described in Section 3.3 of the main article. Lastly, Table 4 is the full version of Table 5 of the main article.

Table 4: List of SB1 from our sample where we found some evidence of orbital motion, and a polynomial was fitted as the orbit could not be sampled or covered adequately.

Cepheid	deg	A_{p2p} (km s^{-1})	ΔT_{p2p} (d)	Trend
SB1s discovered in the current work				
AQ Pup	3	3.32	2500	up
ASAS J064553+1003.8	3	1.11	2347	down
ASAS J103158-5814.7	4	13.95	3658	down
ASAS J155847-5341.8	1	0.58	3587	down
ASAS J174108-2328.5	1	0.38	2533	up
DR Vel	2	0.25	1657	down
OX Cam	1	0.87	2549	down
RY Sco	1	0.61	2646	up
RY Vel	6	2.54	2126	up
SX Vel	1	0.28	2140	up
V0391 Nor	2	2.52	3511	down
V0492 Cyg	2	2.03	1895	up
V0827 Cas	1	0.31	2568	up
V1162 Aql	2	0.24	656	up
V1803 Aql	1	2.44	3635	down
V2475 Cyg	2	5.71	3404	down
Literature-known SB1s				
AD Pup	4	1.45	818	down
AH Vel	1	1.74	2126	up
AQ Car	1	0.72	2817	down
AW Per	1	3.95	2567	down
FR Car	1	0.35	2116	up
KN Cen	3	2.83	2857	down
LR TrA	3	3.52	3664	up
RV Sco	2	5.34	3429	up
RW Cam	1	1.69	2680	up
RX Aur	1	0.63	1224	up
T Mon	1	1.20	3841	up
UX Per	2	7.21	3657	down
UZ Sct	4	4.61	1426	up
XZ Car	1	0.63	3658	up

Notes. Column 2 represents the degree of polynomial used in our analysis, Column 3 lists the peak-to-peak amplitude of the (linear or nonlinear) v_γ variation and Column 4 lists the timeline (in days) over which this amplitude was computed. The last column indicates the direction of the trend, up for increasing velocity, down for decreasing.

4. RV template fits after zero-point offset correction for sample stars with no signs of SB1

Figures 48 and 48 showcase the long-terms trends in v_γ for sample stars where we find no signs of binarity through the RVTF analysis of Section 3.4 of the main article.

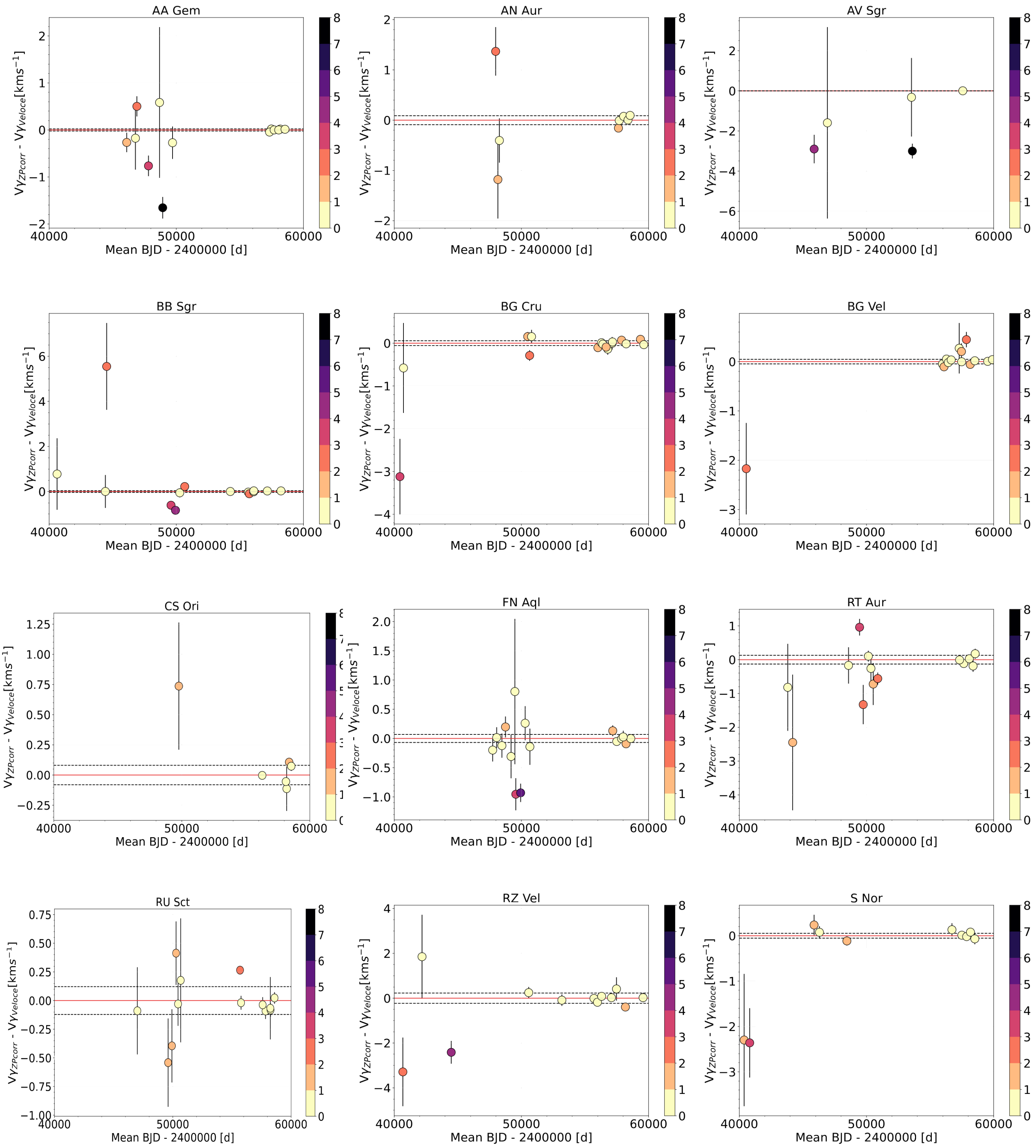

Fig. 48: contd. on the next page

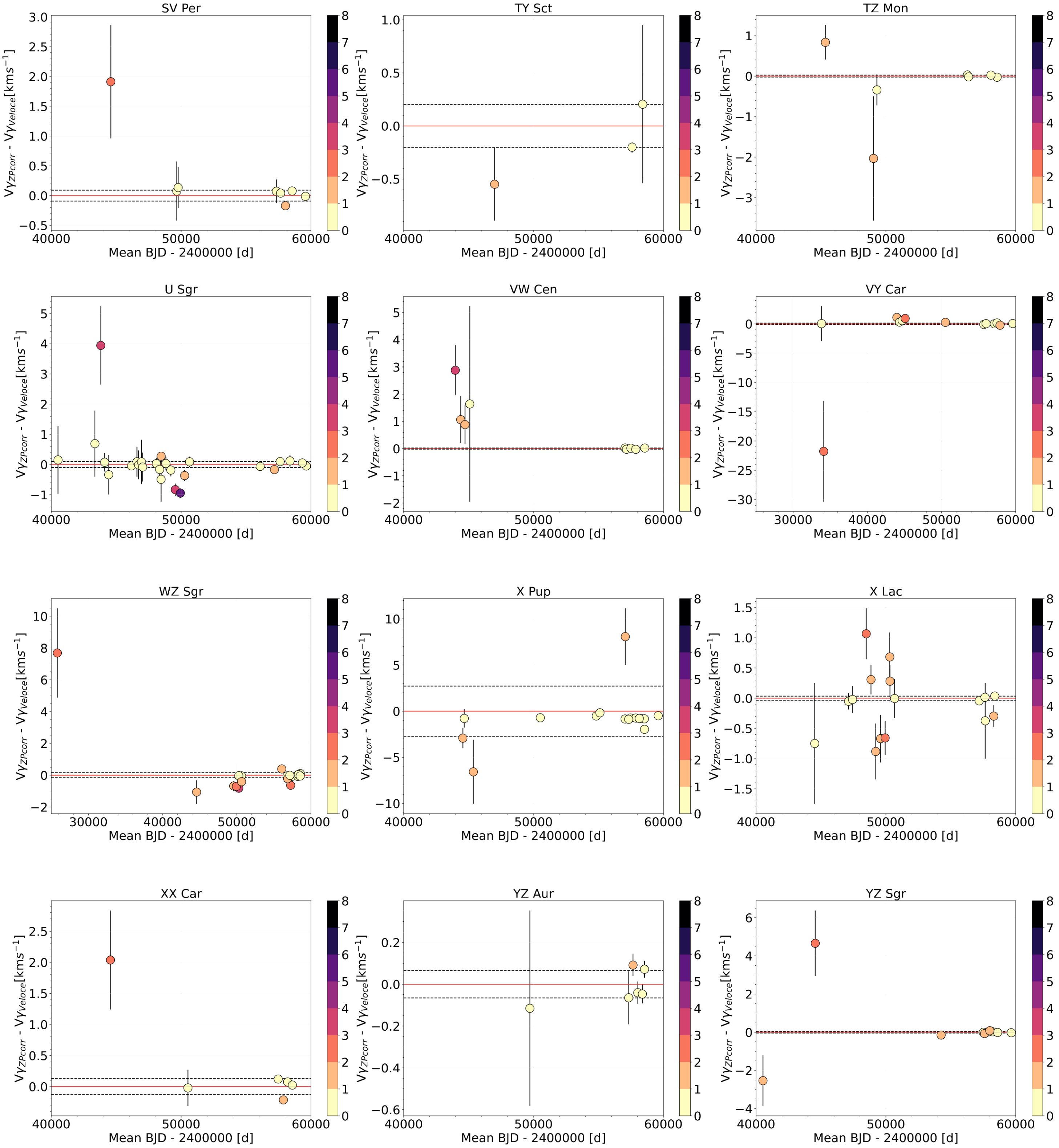

Fig. 48: Zero-point corrected Δv_γ for stars within VELOCE with no signs of SB1 from their v_γ RVTF analysis (contd. on the next page). The dotted lines mark the standard deviation of the $v_{\gamma\mathrm{VELOCE}}$. The color bar represents the $\mathrm{S/N}_{\mathrm{SB1}}$ of the various v_γ measurements where the $\mathrm{S/N}_{\mathrm{SB1}}$ was calculated as described in the text.

5. Gaia astrometry

In Table 5, we present all the *Gaia* RUWE and PMa flags used in this study for all our sample stars.

Table 5: *Gaia* astrometry and PMa tags for the confirmed SB1 Cepheids within VELOCE. Here, binary flag of "1" means that the star was flagged as binary through PMa, and binary flag of "0" means the PMa did not detect them as binaries. These *Gaia* parameters are discussed in Section 5.3 of the main article.

Star	RUWE	Bin flag from PMa	Star	RUWE	Bin flag from PMa	Star	RUWE	Bin flag from PMa
SB1 with Orbits			SB1 with Trends			SB1 with RVTF-Yes		
ASAS J064540+0330.4			AD Pup	1.3621	0	β Dor	4.5348	0
ASAS J084951-4627.2	1.0863		AH Vel	0.8293	1	η Aql	2.5610	0
ASAS J100814-5856.6	1.1193		AQ Pup	1.1803	0	CD Cyg	1.0070	0
ASAS J174603-3528.1	0.6934		AQ Car	1.0672	0	RS Ori	1.1190	0
AX Cir	7.8052		ASAS J064553+1003.8	1.4999		SS CMa	1.1134	0
BP Cir	1.0495		ASAS J103158-5814.7	0.8688		SZ Aql	0.9400	0
δ Cep	2.7131		ASAS J155847-5341.8	0.8680		SZ Cyg	0.9560	0
DL Cas	1.8830	0	ASAS J174108-2328.5	0.7577		V0340 Ara	0.9316	0
FF Aql	1.0554	1	AW Per	1.1555	1	V0402 Cyg	0.9200	0
FN Vel	1.6964	0	DR Vel	1.0050		V0916 Aql	0.9160	
FO Car	0.9023		FR Car	1.0235	0	VY Sgr	0.8057	
GX Car	1.0176	1	KN Cen	1.0336	0	X Cyg	1.2774	1
IT Car	1.0755	1	LR TrA	0.9513	1			
MU Cep	0.9928		OX Cam	0.9844				
MY Pup	1.0087	0	RY Vel	1.0752	0			
NT Pup	0.9861		RX Aur	0.9821	1			
R Cru	1.1609		RV Sco	0.8048	1			
R Mus	1.0742	1	RW Cam	8.0130	1			
S Mus	4.4948	1	RY Sco	0.7326	0			
S Sge	4.0033	1	SX Vel	1.0222	0			
SU Cyg	3.4429	0	T Mon	1.7239	1			
SY Nor	1.5525	0	UX Per	1.1668	1			
TX Mon	1.6886	1	UZ Sct	0.9132				
U Vul	2.8825	1	V0391 Nor	0.8320				
V0407 Cas	0.8948		V0492 Cyg	0.9966				
V0659 Cen	2.9896	1	V0827 Cas	1.1600				
V1334 Cyg	2.7684	1	V1162 Aql	0.9524	0			
VY Per	1.1544		V1803 Aql	0.9415				
VZ Pup	1.2366	0	V2475 Cyg	0.9943				
W Sgr	3.9524	0	XZ Car	1.0491	0			
XX Cen	1.2385	0						
YZ Car	1.1658	0						
Z Lac	1.0548	0						

6. SU Cyg RVTF

In Table 6, we present the zero-point corrected v_γ residuals (ϵv_γ) of SU Cyg. The details of how these were obtained are provided in Section 4.5 of the main article.

Table 6: RV data used for the V+L orbit estimation of SU Cyg.

Reference	BJD (d)	ϵv_γ ($\mathrm{km\,s^{-1}}$)	$\sigma\epsilon v_\gamma$ ($\mathrm{km\,s^{-1}}$)	Reference	BJD (d)	ϵv_γ ($\mathrm{km\,s^{-1}}$)	$\sigma\epsilon v_\gamma$ ($\mathrm{km\,s^{-1}}$)	Reference (d)	BJD ($\mathrm{km\,s^{-1}}$)	ϵv_γ ($\mathrm{km\,s^{-1}}$)	$\sigma\epsilon v_\gamma$
Ba87	43 616.98	−25.28	5.34	Bo19	56 566.33	4.12	2.06	Go92	50 705.31	−14.31	0.74
Ba87	43 617.98	−29.49	5.34	Bo19	56 898.52	−55.52	0.39	Go92	50 707.32	−16.54	0.81
Ba87	43 618.97	−18.86	5.34	Bo19	56 899.57	−57.23	0.39	Go92	50 708.35	−21.89	0.88
Ba87	43 620.99	−33.88	5.34	Bo19	56 900.44	−56.70	0.39	Go92	50 708.35	−21.97	0.79
Ba87	43 622.96	−36.96	5.34	Bo19	56 901.57	−57.04	0.39	Go92	50 709.29	−16.26	0.76
Ba87	43 683.86	−44.62	4.50	Go92	50 236.43	−31.47	1.11	Go92	50 711.25	−15.71	0.78
Ba87	43 683.86	−38.26	4.50	Go92	50 238.40	−31.79	1.11	Go92	50 713.28	−16.36	0.75
Ba87	43 684.84	−41.70	4.50	Go92	50 245.48	−36.12	1.15	Go92	50 714.38	−16.70	0.77
Ba87	43 684.84	−36.56	4.50	Go92	50 246.51	−36.22	1.20	Go92	50 715.25	−13.86	0.81
Ba87	43 684.85	−37.22	4.50	Go92	50 247.50	−32.82	1.22	Go92	50 716.29	−20.98	0.87
Ba87	43 685.77	−39.75	4.50	Go92	50 248.47	−35.83	1.16	Go92	50 718.27	−16.77	0.77
Ba87	43 686.81	−41.03	4.50	Go92	50 255.42	−38.30	0.78	Go92	50 719.24	−13.29	0.80
Ba87	43 688.84	−39.13	4.50	Go92	50 257.46	−36.84	0.79	Go92	50 719.25	−13.31	0.75
Ba87	43 713.94	−54.46	4.50	Go92	50 259.41	−38.76	0.76	Go92	50 720.34	−17.83	0.81
Ba87	43 821.58	−31.42	4.14	Go92	50 261.41	−39.11	0.80	Go92	50 726.33	−20.37	0.81
Ba87	43 822.57	−29.65	4.14	Go92	50 264.48	−40.48	0.78	Go92	50 727.29	−16.22	0.87
Ba87	43 825.67	−28.00	4.14	Go92	50 265.41	−40.77	0.86	Go92	50 728.33	−21.40	0.80
Ba87	44 044.87	−9.43	4.15	Go92	50 275.46	−45.78	1.29	Go92	50 729.31	−18.55	0.85
Ba87	44 045.89	−5.06	4.15	Go92	50 276.43	−47.12	1.27	Go92	50 730.30	−20.42	0.82
Ba87	44 046.88	−7.48	4.15	Go92	50 277.41	−46.35	1.39	Go92	50 731.25	−22.28	0.79
Ba87	44 059.87	−12.19	4.15	Go92	50 278.42	−47.40	1.30	Go92	50 732.23	−20.55	0.83
Ba87	44 060.89	−8.55	4.15	Go92	50 279.44	−46.92	1.29	Hermes	55 896.32	−21.12	0.60
Ba87	44 063.89	−5.09	4.15	Go92	50 280.41	−48.98	1.33	Hermes	55 896.32	−21.06	0.60
W89	43 378.67	5.42	4.11	Go92	50 281.38	−49.72	1.31	Hermes	55 897.32	−20.75	0.59
W89	43 378.68	−2.60	4.11	Go92	50 284.42	−36.17	1.35	Hermes	55 897.32	−20.72	0.59
W89	43 378.76	−1.49	4.11	Go92	50 285.37	−52.24	1.35	Hermes	55 898.32	−20.20	0.59
W89	43 378.76	2.46	4.11	Go92	50 333.33	−53.54	2.07	Hermes	55 898.32	−20.22	0.59
W89	43 378.82	5.24	4.11	Go92	50 342.26	−50.21	2.05	Hermes	55 900.35	−19.65	0.60
W89	43 378.83	0.78	4.11	Go92	50 345.30	−48.24	2.06	Hermes	55 900.36	−19.76	0.60
W89	43 381.86	2.54	4.11	Go92	50 619.49	1.15	4.76	Hermes	56 091.50	−3.43	0.20
W89	43 381.86	6.49	4.11	Go92	50 621.52	−2.18	4.76	Hermes	56 092.57	−3.58	0.24
W89	43 384.67	3.01	4.11	Go92	50 623.49	−7.05	4.76	Hermes	56 093.48	−3.50	0.22
W89	43 384.67	2.18	4.11	Go92	50 652.37	−6.34	0.95	Hermes	56 097.61	−3.36	0.22
W89	43 384.82	2.26	4.11	Go92	50 653.49	−4.95	0.93	Hermes	56 098.61	−2.52	0.24
W89	43 384.83	1.53	4.11	Go92	50 655.42	−8.75	0.93	Hermes	56 099.60	−2.63	0.25
W89	43 385.65	−1.67	4.11	Go92	50 658.47	−12.37	0.93	Hermes	58 070.37	−32.19	0.54
W89	43 386.65	6.80	4.11	Go92	50 662.39	−9.66	0.98	Hermes	58 071.37	−32.02	0.57
W89	43 387.66	2.96	4.11	Go92	50 663.44	−7.67	0.98	Hermes	58 071.38	−31.40	0.55
W89	43 388.63	0.29	4.11	Go92	50 667.47	−8.53	0.89	Hermes	58 073.34	−31.03	0.55
Bo19	56 500.52	1.37	2.06	Go92	50 668.48	−10.31	0.97				
Bo19	56 501.57	1.52	2.06	Go92	50 669.46	−6.40	0.97				
Bo19	56 504.60	1.61	2.06								
Bo19	56 505.51	2.06	2.06								
Bo19	56 563.32	4.52	2.06								
Bo19	56 565.43	2.33	2.06								

Notes. The column labeled "Reference" lists the sources of various RV datasets, with corresponding abbreviations as follows: , Ba87 for Barnes et al. (1987), W89 for Wilson et al. (1989), Bo19 for Borgniet et al. (2019), Go92 for Gorynya et al. (1992). In column 2 is the Barycentric Julian Date (BJD) of the observation, in column 3 is the residuals between the measurement and the VELOCE template (ϵv_γ) after applying the zero-point offset (shifted according to the phase shift of the epoch) v_γ residuals.Finally, in column 4 we present the uncertainty on the zero-point corrected ϵv_γ.

References

Anderson, R. I. 2013, PhD thesis, Université de Genève
Anderson, R. I. 2019, A&A, 623, A146
Anderson, R. I., Casertano, S., Riess, A. G., et al. 2016, ApJS, 226, 18
Anderson, R. I., Sahlmann, J., Holl, B., et al. 2015, ApJ, 804, 144
Anderson, R. I., Viviani, G., Shetye, S. S., et al. 2024, A&A, 686, A177
Barnes, III, T. G., Moffett, T. J., & Slovak, M. H. 1987, ApJS, 65, 307
Bersier, D. 2002, ApJS, 140, 465
Bersier, D., Burki, G., Mayor, M., & Duquennoy, A. 1994, A&AS, 108, 25
Borgniet, S., Kervella, P., Nardetto, N., et al. 2019, A&A, 631, A37
Ekström, S., Georgy, C., Eggenberger, P., et al. 2012, A&A, 537, A146
Evans, N. R. 1991, ApJ, 372, 597
Evans, N. R. 1992, ApJ, 384, 220
Evans, N. R. 1994, ApJ, 436, 273
Evans, N. R. 1995, ApJ, 445, 393
Evans, N. R., Szabados, L., & Udalska, J. 1990, PASP, 102, 981
Evans, N. R. & Udalski, A. 1994, AJ, 108, 653
Gallenne, A., Kervella, P., Borgniet, S., et al. 2019, A&A, 622, A164
Gallenne, A., Monnier, J. D., Mérand, A., et al. 2013, A&A, 552, A21
Gieren, W. 1982, ApJS, 49, 1
Gorynya, N. A., Irsmambetova, T. R., Rastorguev, A. S., & Samus, N. N. 1992, Soviet Astronomy Letters, 18, 316
Gorynya, N. A., Rastorguev, A. S., & Samus, N. N. 1996a, Astronomy Letters, 22, 33
Gorynya, N. A., Samus', N. N., Rastorguev, A. S., & Sachkov, M. E. 1996b, Astronomy Letters, 22, 175
Griffin, R. F. 2016, The Observatory, 136, 209
Kovtyukh, V., Szabados, L., Chekhonadskikh, F., Lemasle, B., & Belik, S. 2015, MNRAS, 448, 3567
Lloyd Evans, T. 1982, MNRAS, 199, 925
Madore, B. F. 1977, MNRAS, 178, 505
Petterson, O. K. L., Cottrell, P. L., & Albrow, M. D. 2004, MNRAS, 350, 95
Pont, F., Mayor, M., & Burki, G. 1994, A&A, 285, 415
Russo, G., Sollazzo, C., & Coppola, M. 1981, A&A, 102, 20
Shetye, S. S., Viviani, G., Anderson, R. I., et al. 2024, arXiv e-prints, arXiv:2405.19840
Szabados, L. 1992, The Observatory, 112, 57
Szabados, L. 1996, A&A, 311, 189
Szabados, L. 2003, Information Bulletin on Variable Stars, 5394
Szabados, L., Anderson, R. I., Derekas, A., et al. 2013a, MNRAS, 434, 870
Szabados, L., Cseh, B., Kovács, J., et al. 2014, MNRAS, 442, 3155
Szabados, L., Derekas, A., Kiss, L. L., et al. 2013b, MNRAS, 430, 2018
Szabados, L. & Pont, F. 1998, A&AS, 133, 51
Turner, D. G., Bryukhanov, I. S., Balyuk, I. I., et al. 2007, PASP, 119, 1247
Wahlgren, G. M. & Evans, N. R. 1998, A&A, 332, L33
Wilson, T. D., Carter, M. W., Barnes, III, T. G., van Citters, Jr., G. W., & Moffett, T. J. 1989, ApJS, 69, 951